University of Groningen

Stabilizing CrO by epitaxial growth

Rogojanu, Oana Corina; Sawatzky, G.A; Tjeng, L.H

IMPORTANT NOTE: You are advised to consult the publisher's version (publisher's PDF) if you wish to cite from it. Please check the document version below.

Document Version
Publisher's PDF, also known as Version of record

Publication date:
2002

Link to publication in University of Groningen/UMCG research database

Citation for published version (APA):
Rogojanu, O. C., Sawatzky, G. A., & Tjeng, L. H. (2002). *Stabilizing CrO by epitaxial growth*. s.n.

Copyright
Other than for strictly personal use, it is not permitted to download or to forward/distribute the text or part of it without the consent of the author(s) and/or copyright holder(s), unless the work is under an open content license (like Creative Commons).

The publication may also be distributed here under the terms of Article 25fa of the Dutch Copyright Act, indicated by the "Taverne" license. More information can be found on the University of Groningen website: https://www.rug.nl/library/open-access/self-archiving-pure/taverne-amendment.

Take-down policy
If you believe that this document breaches copyright please contact us providing details, and we will remove access to the work immediately and investigate your claim.

Downloaded from the University of Groningen/UMCG research database (Pure): http://www.rug.nl/research/portal. For technical reasons the number of authors shown on this cover page is limited to 10 maximum.

Download date: 05-05-2023

Chapter 4

O_2 and O_3 assisted chromium oxides growth

4.1 Introduction

After the NO_2 - assisted chromium oxide growth, O_2 and O_3 were used next as oxidizing agents in order to avoid the nitrogen contaminations in the samples at low gas pressure, when approaching the chemical composition of stoichiometric CrO.

In this chapter we discuss the preparation of O_2 and O_3 - assisted samples, using in general the growth conditions that have been established in the previous chapter. The sample characterization was done by RHEED, LEED and XPS *in situ*, followed by RBS, XRD and XAS *ex situ*. RHEED and XPS were used for all the grown samples, while the other techniques were used on some selected samples. Selection of which was made based on the crystal structure and/or sample stoichiometry.

4.2 O_2 assisted growth

Following the recipe found in the case of NO_2 assisted MBE growth of chromium oxides, oxygen assisted samples were deposited on $MgO(100)$ and $MnO(100)$ substrates using a chromium metal deposition rate of $\approx 1.3\text{Å}/\min$ and $400°\text{C}$ substrate temperature. The O_2 buffer volume pressure was varied from 0.5×10^{-4} mbar to 6×10^{-4} mbar when using MgO substrates, and these pressures are listed in the following table together with the corresponding background pressures in the growth chamber before starting the growth, just after the O_2 P_{buf} was set to the

desired value "$P_{chamber}$ when staring the growth", and almost in the end of the growth "$P_{chamber}$ after ≈ 25 min. of growth".

P_{buf} (mbar)	$P_{chamber}$ when staring the growth (mbar)	$P_{chamber}$ after ≈ 25 min. of growth (mbar)
0.5×10^{-4}	8×10^{-9}	9×10^{-9}
1×10^{-4}	1.2×10^{-8}	1.7×10^{-8}
1.5×10^{-4}	2.4×10^{-8}	4.6×10^{-8}
2×10^{-4}	2.3×10^{-8}	7.2×10^{-8}
3×10^{-4}	3.5×10^{-8}	2×10^{-7}
4×10^{-4}	5.3×10^{-8}	2.7×10^{-7}
6×10^{-4}	1.2×10^{-7}	4.7×10^{-7}

After the sample growth is started, $P_{chamber}$ is rising slightly due to saturation of the growth chamber while the oxidizing agent is fed with a constant flow. Also the chromium K-cell outgassing is contributing a bit to this variation of $P_{chamber}$ during growth.

For the samples grown on MnO substrates P_{buf} used were: 1×10^{-4}, 1.5×10^{-4} and 2×10^{-4} mbar. All the sample deposition times were 30 minutes. The measurements performed on these samples were RHEED - during growth and XPS - immediately after the growth, and the results of these measurements will be discussed in the following subsections.

4.2.1 *In situ* structural analysis: RHEED

Figure 4.1 show the RHEED patterns of (a) a cleaned $MgO(100)$ substrate and some of the samples grown on MgO substrates under the following O_2 buffer volume pressures: (b) 0.5×10^{-4} mbar, (c) 1×10^{-4} mbar, (d) 1.5×10^{-4} mbar, (e) 2×10^{-4} mbar, (f) 6×10^{-4} mbar. Due to severe charging problems, no good data were recorded for P_{buf}: 3×10^{-4} and 4×10^{-4} mbar. All the images of the grown samples were recorded at the end of each growth with an electron beam energy of 15 keV and with the incident beam along a [100] direction of the substrate.

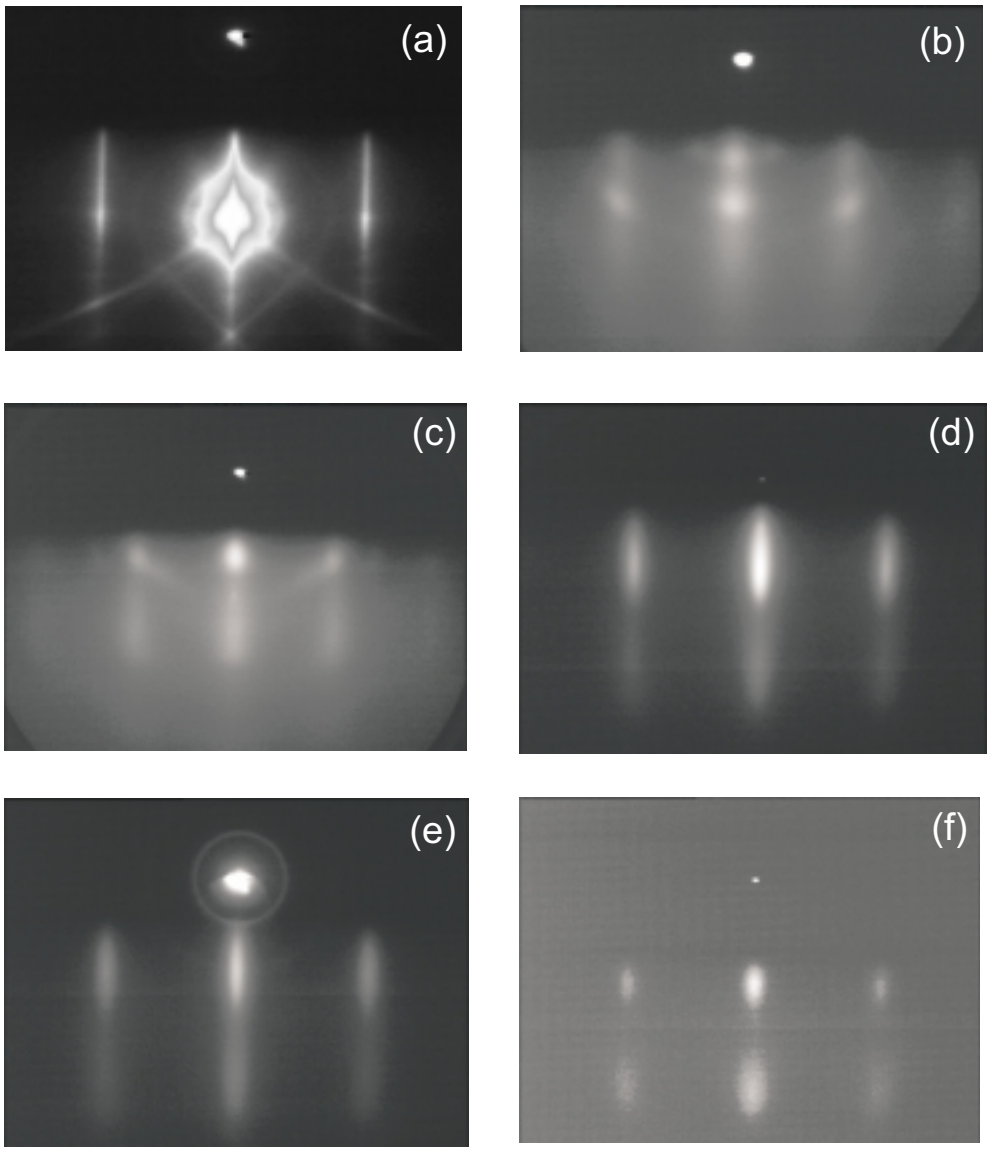

FIGURE 4.1. RHEED patterns of (a) $MgO(100)$ substrate and grown samples on $MgO(100)$ at 400°C, O_2 assisted with buffer volume pressures: (b) 0.5×10^{-4} mbar, (c) 1×10^{-4} mbar, (d) 1.5×10^{-4} mbar, (e) 2×10^{-4} mbar, (f) 6×10^{-4} mbar.

The distance between the lines is not the same for all the pictures due to slightly different positions of the CCD camera when the pictures were taken.

For $P_{buf} \geq 1.5 \times 10^{-4}$ mbar the film pattern looked similar to that of the substrate, having the characteristic rocksalt $(\overline{2}, 0)$, $(0, 0)$ and $(2, 0)$ diffraction rods. The surfaces seem to be relatively smooth in the cases of P_{buf} is 1.5×10^{-4} and 2×10^{-4} mbar. For $P_{buf} \geq 3 \times 10^{-4}$ mbar the rods are split into spots indicating surface roughening. The samples grown at $P_{buf} = 0.5 \times 10^{-4}$ mbar and 1×10^{-4} mbar transmission patterns developed directly after starting the growth, ending with very diffuse rocksalt patterns combined with polycrystalline features and high backgrounds, indicating deterioration of the crystalline structure in these cases, and also some extra spots probably due to the growth of some epitaxial chromium metal.

RHEED intensity oscillations in the specularly reflected beam were obtained for P_{buf}: 1.5×10^{-4} mbar (Fig. 4.3 a) and 2×10^{-4} mbar with a period of $47.3\,\mathrm{sec}\,/ML$ and a damping in the oscillatory behavior at the end of the growth; for 3×10^{-4} mbar and 4×10^{-4} mbar, a few oscillations in the early stages of growth with a period of $\approx 42.5\,\mathrm{sec}\,/ML$. The ratio of these two periods is very close to 8/9, the expected periods ratio of $Cr_{0.67}O$ to $Cr_{0.75}O$ phases. For the sample grown at $P_{buf} = 1 \times 10^{-4}$ mbar three RHEED intensity oscillations were obtained with a separation of ≈ 56 seconds. From the ratio of this period with the previous ones, the chemical composition of the sample is estimated to be $\approx Cr_{0.9}O$. Further investigations on the chemical composition of the samples was done by XPS.

The chromium oxide deposition on $MnO(100)$ substrates proved to give similar results to the growth on $MgO(100)$ substrates, as far as RHEED data are concerned. Figure 4.2 a is a RHEED pattern of a clean MnO substrate taken before the growth of one of the samples. The RHEED gun settings were the same as for the MgO substrate case. The characteristic rocksalt pattern with the $(\overline{2}, 0)$, (0,0) and (2,0) streaks can be recognized, but they are less sharp and intense than those of the MgO substrate, lying also on a higher intensity background. This is probably due to the fact that MgO (transparent crystal) has much less defects than MnO (opaque and very dark color crystal). More important is that MgO substrates have excellent surfaces after cleave, while for MnO the mosaicity of the substrate can be seen with the naked eye after the cleave.

In figure 4.2 (a) the Kikuchi lines and the intense spot of the reflected electrons on the MnO surface are also visible. Next, figure 4.2 (b), (c) and (d) show the RHEED images of the grown samples on MnO substrates at 400°C and O_2 buffer

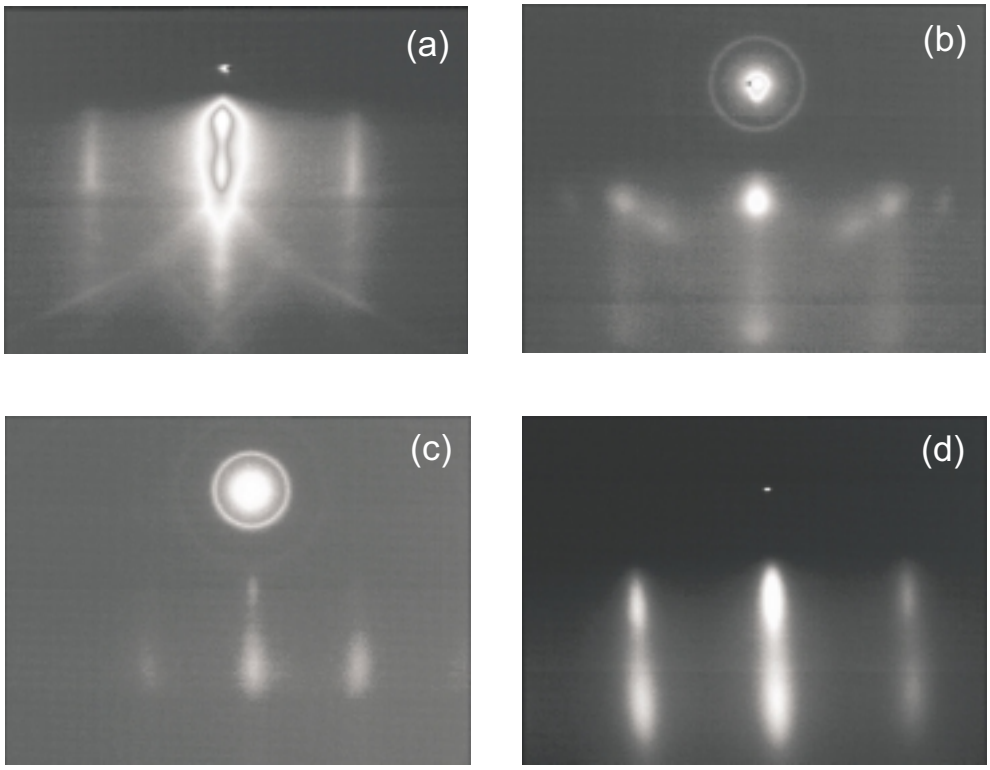

FIGURE 4.2. RHEED patterns of (a) $MnO(100)$ substrate and grown samples on $MnO(100)$ at 400°C, O_2 assisted with buffer volume pressures: (b) 1×10^{-4} mbar, (c) 1.5×10^{-4} mbar, (d) 2×10^{-4} mbar.

volume pressures of 1×10^{-4} mbar, 1.5×10^{-4} mbar and 2×10^{-4} mbar respectively. As for the growth on MgO substrates, $P_{buf} = 1\times10^{-4}$ mbar of O_2 seems to be not enough for growing single-crystal chromium oxide films. The transmission spots appear in the beginning of the film deposition and then slowly the polycrystalline features develop. No oscillations in the reflected beam intensity were obtained in this case. The intensity just drops rapidly in the beginning of the growth. For oxygen P_{buf} of 1.5×10^{-4} and 2×10^{-4} mbar the RHEED patterns indicated an epitaxial growth on the MnO substrates, with relatively rough surfaces, but still in rocksalt crystalline arrangement. RHEED intensity oscillations for $P_{buf} =$

2×10^{-4} mbar sample are shown in figure 4.3 b. The damping in the oscillatory behavior indicate also that in the second half of the deposition time, the growth mode of this sample is three dimensional, with an increased surface roughness.

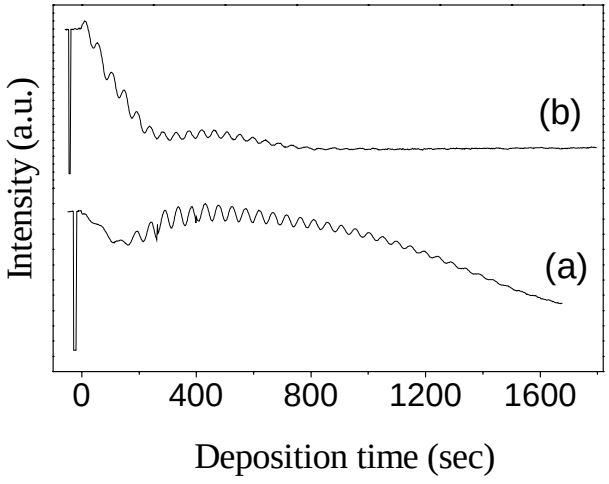

FIGURE 4.3. Oscillations in the intensity of the specularly reflected RHEED beam, as a function of the deposition time for samples grown (a) on $MgO(100)$ substrate at O_2 $P_{buf} = 1.5 \times 10^{-4}$ mbar, (b) on $MnO(100)$ substrate at O_2 $P_{buf} = 2 \times 10^{-4}$ mbar.

The oscillations presented in figure 4.3 are the best obtained for the O2 - assisted growth and they were recorded in the same way as described for the RHEED intensity oscillations of the NO_2 - assisted samples (subsection 3.3.1). The intensity was also normalized and the deep minima correspond to the moment when the RHEED beam was shuttered. The actual sample deposition starts at time = 0 seconds. The oscillations are evenly spaced, but compared with the ones obtained for the NO_2 - assisted growth (figure 3.3) they have smaller amplitude and a much faster damping. This fact indicates that the growth is far better for the NO_2 - assisted samples than for the O_2 - assisted ones.

4.2.2 Chemical composition

After a brief investigation of the crystal quality of the samples with RHEED, XPS was used to check the chemical composition of the layers. First a broad scan was taken in each case, in order to check for the possible contaminations in the samples. As expected, no nitrogen contamination was found this time, and the surfaces were also carbon - free. No magnesium signal coming from the substrate could be detected. Next, a scan including the Cr 2p and O 1s core level peaks was measured. Oxygen is the only anion in the sample, so the chemical composition x of the Cr_xO was determined this time from the ratio of the Cr 2p and O 1s spectral weights. As in the case of NO_2 - assisted growth, the reference sample was the Cr_2O_3 grown on sapphire presented in section 3.4, having a ratio of Cr 2p vs O 1s of 2.92. The results in the figure 4.4 are for the samples which were presented in the beginning of this chapter. The chemical composition x is plotted as a function of the oxygen buffer volume pressure.

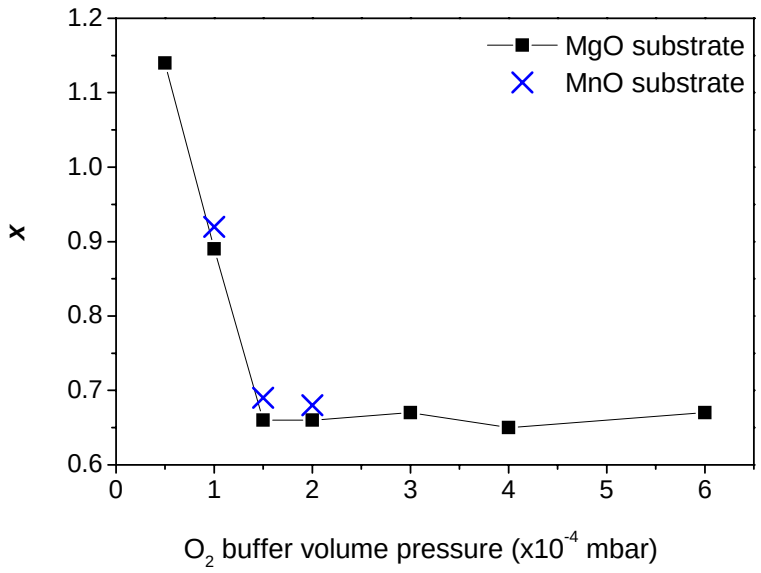

FIGURE 4.4. Chemical composition x of the Cr_xO samples as a function of the O_2 buffer volume pressures as determined from XPS spectra. The reference is Cr_2O_3 grown on $Al_2O_3(0001)$.

From this plot it can be seen that x is close to one for the samples grown at $P_{buf} \leq 1 \times 10^{-4}$ mbar, samples which proved to have poor crystalline order. It is possible that at these low pressures a chromium-metal / chromium oxide phase separated film is being formed.

For the rest of the samples grown at $P_{buf} \geq 1.5 \times 10^{-4}$ mbar, the chemical composition is very close to Cr_2O_3, but surprisingly, they all have rocksalt structures. This indicates that the oxygen sublattice has a rocksalt arrangement, and that in the chromium sublattice vacancies are present, but not in an ordered way.

4.2.3 Reconstruction seen by RHEED and LEED

Next we will discuss RHEED and LEED data of a sample grown with a very high O_2 pressure, which showed a different crystal structure than rocksalt.

The sample was grown on $MgO(100)$ substrate, at 600°C and $P_{buf} = 12.5 \times 10^{-4}$ mbar, leading to a background pressure in the chamber of $\approx 1 \times 10^{-6}$ mbar. In fact, three samples were grown in these conditions, but having different deposition times: 165 seconds, 1200 seconds and 4800 seconds respectively. The RHEED patterns of the three samples (Figure 4.5 b, c and d) are compared with a clean MgO pattern (Figure 4.5 a). It is evident from the pictures that the crystal structure is not rocksalt, and moreover, it is changing as a function of the deposition time.

To follow better this point, the development of the RHEED pattern of the thickest sample is presented in the top most picture of the figure 4.5, composed of a sequence of horizontal line-scans in a box perpendicular to the diffraction rods, as a function of deposition time. The arrows above the picture indicate the times when the RHEED images a, b, c and d were taken (for b and c- when also the growth was stopped). In the beginning, before deposition starts, a couple of MgO images were taken, and there the $(\bar{2}, 0)$, (0,0) and (2,0) features corresponding to the rocksalt diffraction rods can be recognized. The $(\bar{2}, 0)$ and (2,0) are sharp and intense, the (0,0) has a spread out intensity due to the extremely intense reflected electrons spot (see fig. 4.5 a). Upon deposition, the narrow $(\bar{2}, 0)$ and (2,0) lines are replaced by broader, but still intense lines. Then two extra lines are visible in between the rocksalt lines for about 250-300 seconds (5-6 monolayers). They are also sharp and have a streaked characteristic (see fig. 4.5 b).

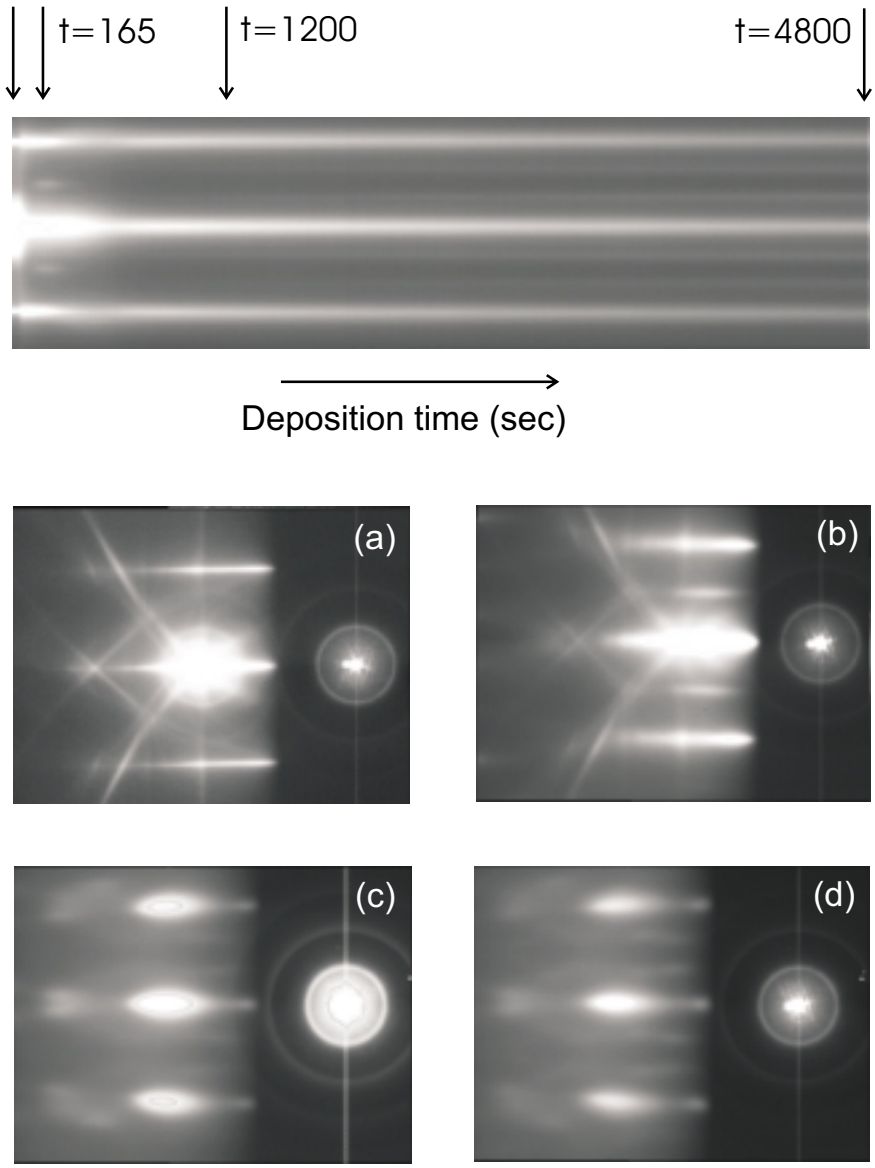

FIGURE 4.5. Top: Development of the RHEED pattern of a sample grown on $MgO(100)$ at 600°C, O_2 assisted with $P_{buf} = 12.5 \times 10^{-4}$ mbar and the deposition time 4800 seconds. RHEED patterns of (a) $MgO(100)$ substrate, and grown samples on MgO at 600°C, O_2 assisted with $P_{buf} = 12.5 \times 10^{-4}$ mbar and the deposition times: (b) 165 seconds, (c) 1200 seconds, (d) 4800 seconds.

At this thickness the Kikuchi lines of the MgO substrate are still visible and the sample seems to be very flat, without transmission features. The extra lines are precisely centered in between the rocksalt lines. As the growth develops the two extra lines disappear and just the rocksalt features remain for another 300-400 seconds, corresponding to a relatively flat film surface. Over 800 seconds of deposition time the surface gets rougher and rougher, (the RHEED streaks transform into transmission spots), and we observe the development of four extra lines as compared with the rocksalt picture, two in between $(\bar{2}, 0)$ and (0,0) streaks, and the other two in between the (0,0) and (2,0) streaks. The distance in between the new features and the rocksalt lines is exactly one third from the (0,0)-(2,0) lines distance. The extra lines remain weak until the end of the growth. Looking in more detail at the pattern in figure 4.5 c and d we could see that in fact, the new extra features have a transmission character, in other words they are a bulk signal: by changing the diffraction angle of the RHEED electrons on the sample surface, the extra features did not change their position but just appeared or disappeared. This was somehow expected due to the increased roughness of the samples. Moreover, in the pictures 4.5 c and d an extra Laue zone is visible where for each rocksalt line from the zeroth order Laue zone appear two lines (it is more clear in 4.5 c).

But before going to the conclusions, let us look at the LEED patterns of the three samples. In figure 4.6 LEED images of the MgO substrate (a and c) are compared with some of the grown samples: (b) and (d) for the 165 seconds deposition time sample, (e) for 1200 seconds sample, and finally (f) for 4800 seconds sample.

The electron beam energies (BE) are indicated on each figure. In figure (b) and (d) the number of spots doubled as compared with the MgO substrate spots and consequently the reciprocal lattice vectors became two times shorter than for MgO. So, in the first stages of growth, the chromium oxide sample has a unit cell two times larger than the MgO unit cell. It could be that this chromium oxide has a spinel crystal structure; or it is just a surface reconstruction with a (2×2) surface unit cell, where one out of four chromium sites is vacant. The chemical composition of chromium oxide having such an ordered defect structure would be $Cr_{0.75}O$. For the spinel type of oxide three compositions are known: the spinel Cr_3O_4 with the lattice constant $a = 8.72$Å, leading to a mismatch with MgO substrate of 3.4%; the gamma phase of Cr_2O_3, again spinel structure with $a = 8.36$Å and a mismatch with MgO of 0.76%; and finally a Cr_2MgO_4 spinel-like oxide with $a = 8.333$Å and a mismatch with MgO of 1.1%.

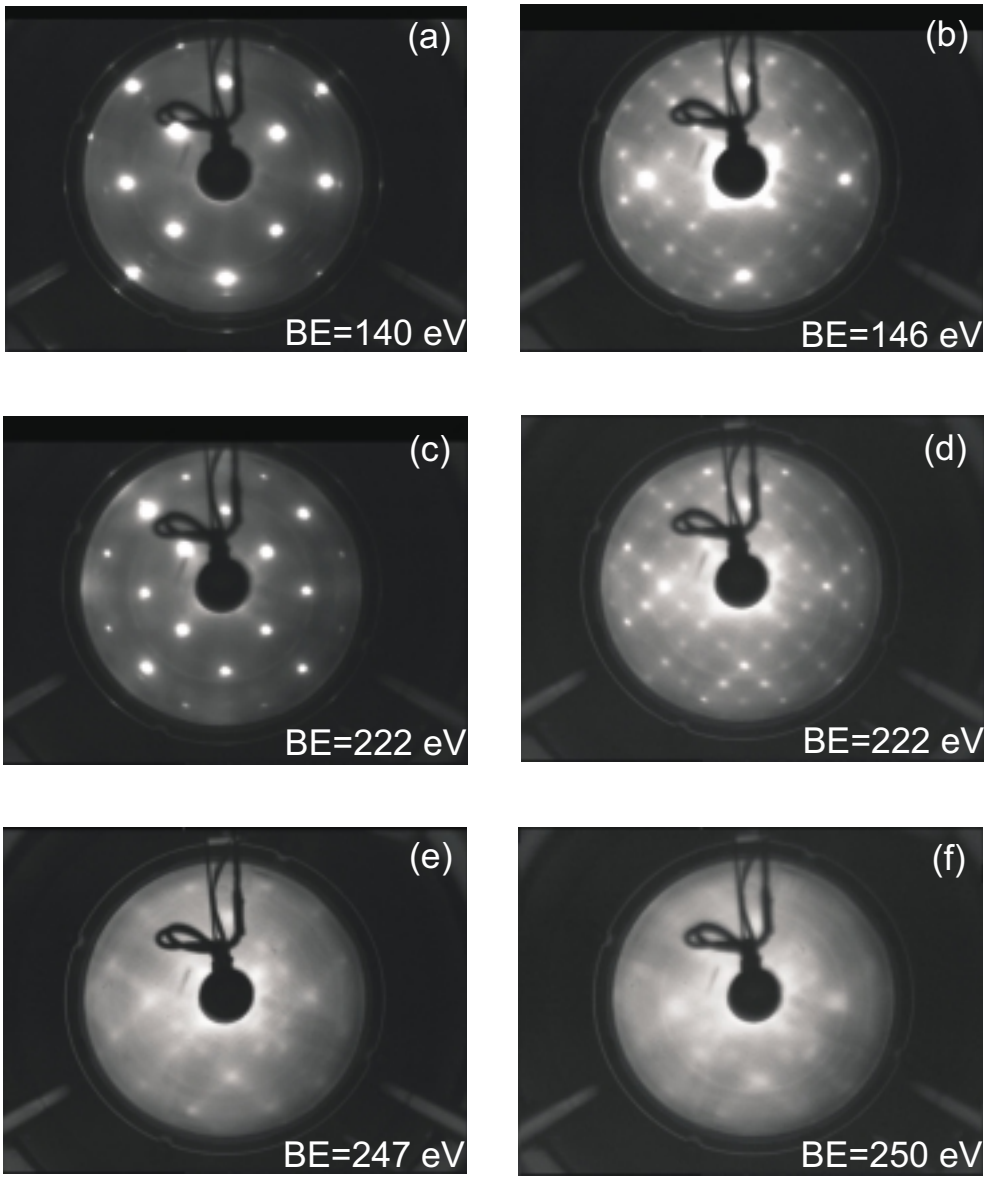

FIGURE 4.6. LEED patterns of (a), (c) $MgO(100)$ substrate, and grown samples on MgO at 600°C, O_2 assisted with $P_{buf} = 12.5 \times 10^{-4}$ mbar and the deposition times: (b), (d) 165 seconds, (e) 1200 seconds, (f) 4800 seconds. The electron beam energy (BE) is indicated on each figure.

The last phase could be formed just if Mg from the substrate would interdiffuse in the chromium oxide overlayer. But with the help of XPS measurements this case could be excluded. This is unlike in the case of Fe_3O_4 growth on MgO where the diffusion of Mg occurs at $\approx 550^{\circ}$C [1]. Further, the sample chemical composition at the very high oxygen pressure used is of $Cr_{0.67}O$, so it is very likely the (2×2) reconstruction with respect to the MgO structure is due to a spinel $\gamma - Cr_2O_3$ phase. For the sample grown 1200 seconds the LEED spots were a bit difficult to distinguish (Fig. 4.6 e), as expected for the rough sample surface. But still, with a careful observation of LEED patterns at different electron beam energies we could conclude that the number of diffraction spots has tripled along the
$< 110 >$ directions, with respect to the MgO unit cell. In other directions no extra diffraction spots could be seen, so we suspect that at this thickness a reconstruction with two domains: (3×1) and (1×3) with respect to the MgO structure was obtained.

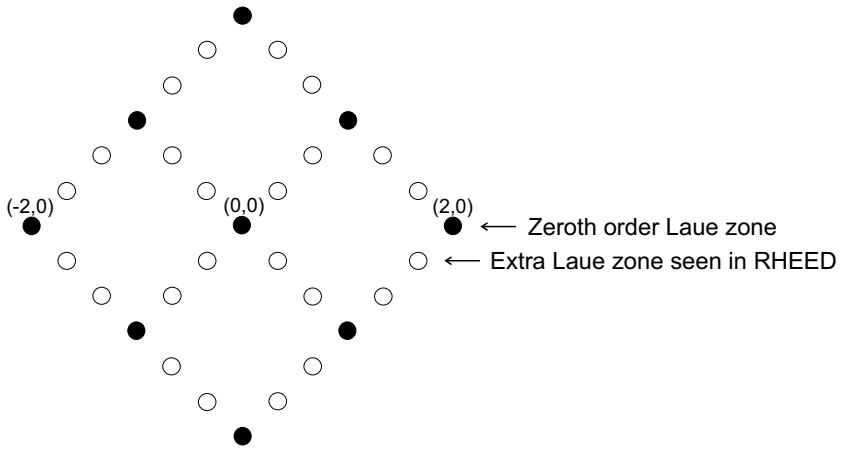

FIGURE 4.7. Schematic drawing of the reconstructed LEED pattern from Figure 4.6.

Figure 4.7 shows a schematic drawing of the reconstructed LEED pattern where the filled circles correspond to the initial rocksalt diffraction spots of the MgO substrate and the open circles to the extra spots appeared for a sample deposition time of 1200 seconds. In the figure the $(\bar{2}, 0)$, (0,0) and (2,0) diffraction spots are also indicated which in the RHEED image are becoming the $(\bar{2}, 0)$, (0,0) and (2,0)

rods, and also the zeroth order Laue zone and the extra Laue zone for the grown sample with respect to the MgO pattern seen in RHEED (fig. 4.5 c). The next Laue zones cannot be seen in RHEED due to a not high enough energy of the electron beam. Due to the two extra lines besides the rocksalt ones in the zeroth order Laue zone which are visible the RHEED pattern, we believe that the film has not just a (3×1) surface reconstruction, but rather an enlarged bulk unit cell, and the RHEED image is a three dimensional collection of (3×1) domains. The extra lines in the zeroth order Laue zone are not visible in LEED probably due to the fact that they are too weak and diffused.

In the LEED pattern of the sample deposited for 4800 seconds (Fig. 4.6 f) the spots are very broad and the background has a very high intensity, so the structure of this sample is not distinguishable from LEED. But due to unchanged symmetry in the RHEED as compared with the thinner, 1200 seconds sample, on the zeroth Laue zone and on the extra Laue zone we can conclude that structure is the same, having a (3×1) domains pattern with respect to MgO structure, but with an increased surface roughness as compared with the thinner sample. A crystal structure consistent with the (3×1) pattern, is a defect rocksalt structure in which one out of three chromium sites is vacant. This means, the new unit cell has the new lattice parameters: $a_1 = a_{MgO}/\sqrt{2}$, $a_2 = 3a_{MgO}/\sqrt{2}$ and $a_3 \approx a_{MgO}$. The chemical composition of the chromium oxide having this structure is $Cr_{0.67}O$.

One may envision that a high substrate temperature during growth (600°C) may help to order the defects in this $Cr_{0.67}O$ films.

4.3 O_3 assisted growth

4.3.1 Sample growth

By using O_3 as oxidizing agent we hoped to overcome the problem of polycrystallinity when the samples approach the chemical composition of chromium monoxide. One may speculate that perhaps the O_3 will react with chromium in such a way that after the reaction only one oxygen radical atom is spilt off and that an oxygen molecule is left behind, and this will not be too reactive with the chromium which is partly oxidized. In this way, one may hope to have an oxygen radical source.

In order to have about the same chromium oxide deposition rate as in the case of NO_2 - and O_2 - assisted growth, the chromium metal flux was set again at approximatively $1.3\mathring{A}/\min$. For the growth study, the substrates used were $MgO(100)$,

$MnO(100)$ and $SrTiO_3(100)$ and the substrate temperatures during growth were: room temperature, 400°C and 600°C. The O_3 buffer volume pressures used are listed in the following table together with the corresponding background pressures in the growth chamber before opening the Cr shutter and almost at the end of the growth, where the sample deposition time was 30 min.

P_{buf} (mbar)	$P_{chamber}$ when staring the growth (mbar)	$P_{chamber}$ after ≈ 25 min. of growth (mbar)
0.75×10^{-4}	1.1×10^{-8}	1.4×10^{-8}
1×10^{-4}	1.5×10^{-8}	2.1×10^{-8}
1.25×10^{-4}	1.6×10^{-8}	3.2×10^{-8}
1.5×10^{-4}	2.1×10^{-8}	4.8×10^{-8}
2×10^{-4}	2.3×10^{-8}	9×10^{-8}
25×10^{-4}	2.4×10^{-7}	1.1×10^{-6}

In the following subsection the *in-situ* characterization by RHEED, LEED and XPS will be discussed. The XPS data were recorded immediately after the growth. Then the results of *ex-situ* measurements: RBS, XRD and XAS, performed on some selected samples, will be shown. For these samples the recipes found by the growth study were applied, their structure was checked by RHEED during growth and the chemical composition by XPS immediately after the growth with a quick Cr 2p - O 1s scan. Other peak scans were not measured for these samples, in order to avoid the post - growth ageing of the samples in the XPS chamber. They were then transported back into the growth chamber where they were capped with about 20 ML of MgO to protect the samples when they were brought into air for ex-situ measurements. The MgO cap layer was grown in the same way as for the NO_2 - assisted samples (see section 3.2), and its stoichiometry was verified by XPS.

4.3.2 *In situ* structural analysis: RHEED and LEED

Figure 4.8 shows the RHEED patterns of (a) a clean $MgO(100)$ substrate, and three of the grown samples on MgO at 400°C and the following O_3 buffer volume pressures: (b) 1×10^{-4} mbar, (c) 1.5×10^{-4} mbar and (d) 2×10^{-4} mbar. The distance between the lines is not the same for all the pictures due to slightly different

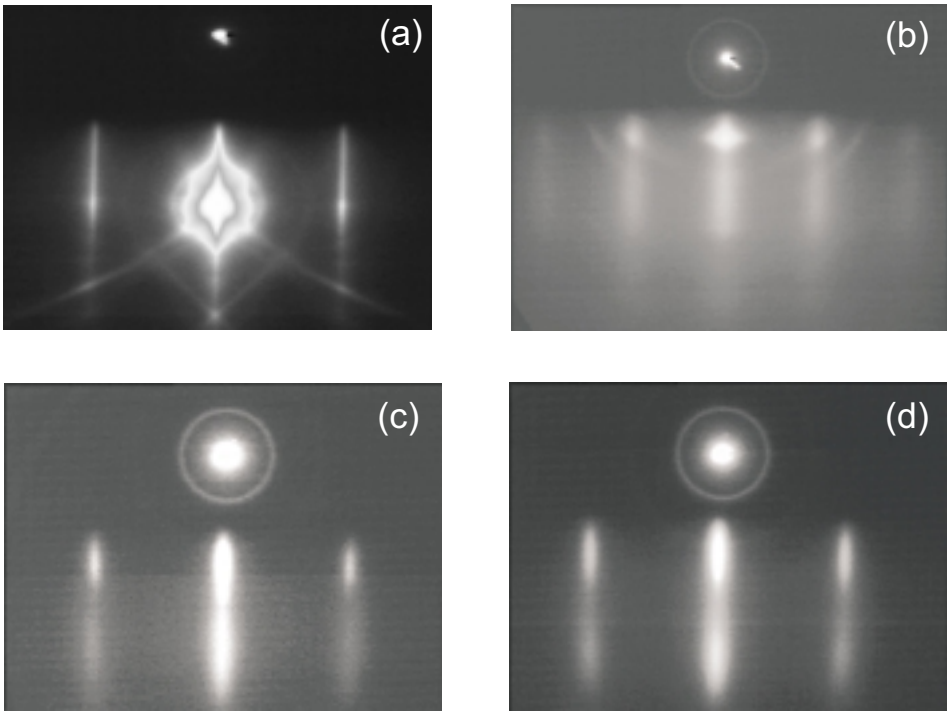

FIGURE 4.8. RHEED patterns of (a) $MgO(100)$ substrate and grown samples on $MgO(100)$ at 400°C, O_3 assisted with buffer volume pressures: (b) 1×10^{-4} mbar, (c) 1.5×10^{-4} mbar, (d) 2×10^{-4} mbar.

positions of the CCD camera when the pictures were taken. The RHEED intensity oscillations in the specularly reflected beam for the latter two samples are presented in figure 4.11 b and d. No oscillations have been observed for the sample grown at $P_{buf} = 1 \times 10^{-4}$ mbar. This fact, together with the polycrystalline features and the very high background intensity in the RHEED pattern, indicates that the sample has a poor crystal quality.

The samples grown at $P_{buf} = 1.5 \times 10^{-4}$ mbar and 2×10^{-4} mbar seem to have rather smooth surfaces in the beginning, but ending with relatively rough surfaces at this thickness.

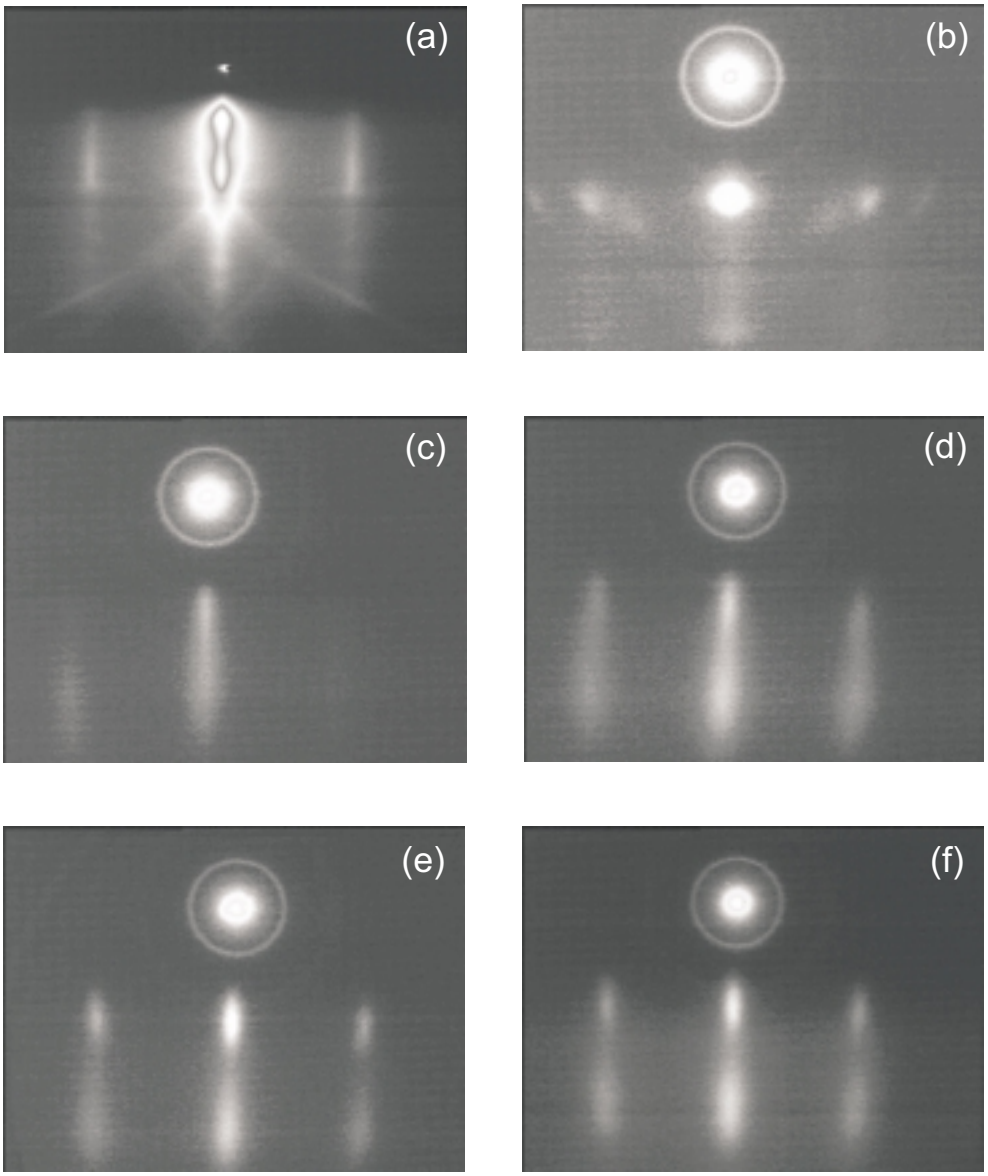

FIGURE 4.9. RHEED patterns of (a) $MnO(100)$ substrate and grown samples on $MnO(100)$ at 400°C, O_3 assisted with buffer volume pressures: (b) 0.75×10^{-4} mbar, (c) 1×10^{-4} mbar, (d) 1.25×10^{-4} mbar, (e) 1.5×10^{-4} mbar, (f) 2×10^{-4} mbar.

In figure 4.9 the RHEED patterns are shown of (a) a clean $Mn(100)$ substrate, and some samples grown on MnO at 400°C, with the O_3 P_{buf} of: (b) 0.75×10^{-4} mbar, (c) 1×10^{-4} mbar, (d) 1.25×10^{-4} mbar, (e) 1.5×10^{-4} mbar, (f) 2×10^{-4} mbar. RHEED oscillations have been observed only for $P_{buf} \geq 1.25 \times 10^{-4}$ mbar samples, and they are presented in figure 4.11 a for the $P_{buf} = 1.25 \times 10^{-4}$ mbar and in 4.11 c for $P_{buf} = 2 \times 10^{-4}$ mbar samples.

For the sample grown at $P_{buf} = 0.75 \times 10^{-4}$ mbar the RHEED pattern consists of transmission spots and polycrystalline features, indicating a very poor crystalline structure for this sample. There are visible also extra spots probably due to the growth of some epitaxial chromium metal. For $P_{buf} = 1 \times 10^{-4}$ mbar sample the RHEED pattern appears to be of a characteristic rocksalt symmetry, although the $(\bar{2}, 0)$ and (2,0) diffraction rods have a very low intensity and a diffuse character making them difficult to see. For higher buffer volume pressures the samples are epitaxial on MnO and in the first half of the total deposition time they grow in a layer-by-layer mode, as the RHEED intensity oscillations suggest. Then, in the second half of the sample deposition time they become rougher, but the films are still epitaxial and have rocksalt crystal structures.

The above-presented results seem to indicate that the O_3 - assisted growth of chromium oxides gives similar results for MgO and MnO substrates. However, an improvement can be observed by using $SrTiO_3(100)$ substrates.

In figure 4.10 the RHEED images are shown of (a) a clean $SrTiO_3$ substrate and samples grown on $SrTiO_3$: (b) at RT and O_3 P_{buf} of 1×10^{-4} mbar, (c) at 400°C and $P_{buf} = 1 \times 10^{-4}$ mbar, (d) at 400°C and $P_{buf} = 1.5 \times 10^{-4}$ mbar, (e) at 400°C and $P_{buf} = 2 \times 10^{-4}$ mbar. RHEED intensity oscillations in the specularly reflected beam were obtained in all these cases, and they are presented in figure 4.11 f, g, h and i.

The RHEED pattern of the substrate shows the $(\overline{2}, 0)$, $(\overline{1}, 0)$, $(0, 0)$, $(1, 0)$ and $(2, 0)$ diffraction rods characteristic for a perovskite structure and the Kikuchi lines. In the first few minutes of the films deposition, this pattern is replaced by characteristic rocksalt features, with the $(\overline{2}, 0)$, $(0, 0)$ and $(2, 0)$ diffraction rods. The growth is of a 2D layer-by-layer type for all the samples.

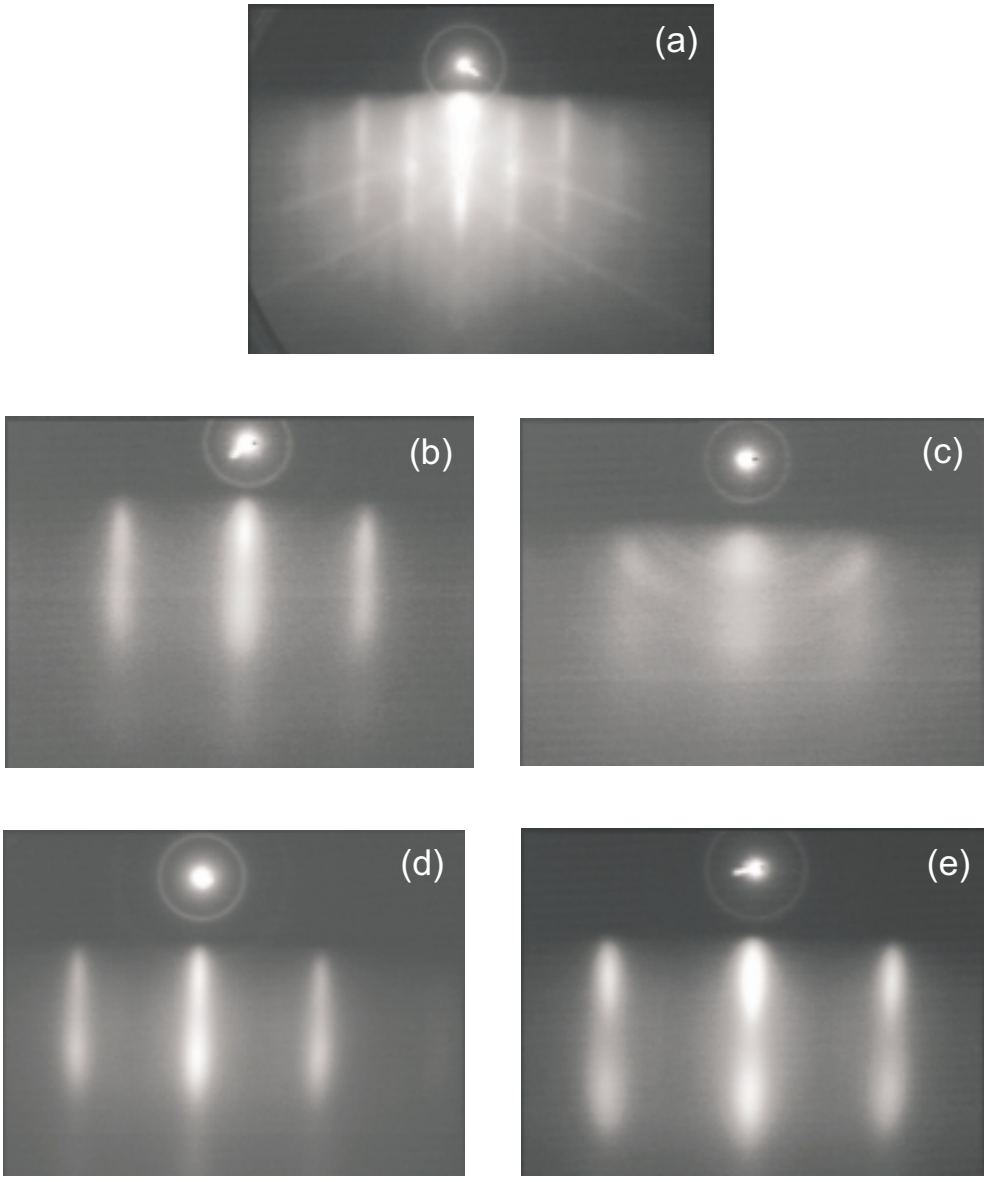

FIGURE 4.10. RHEED patterns of (a) $SrTiO_3(100)$ substrate and grown samples on $SrTiO_3(100)$, O_3 assisted: (b) at RT and $P_{buf} = 1 \times 10^{-4}$ mbar, (c) at $400°$C and $P_{buf} = 1 \times 10^{-4}$ mbar, (d) at $400°$C, $P_{buf} = 1.5 \times 10^{-4}$ mbar, (e) at $400°$C, $P_{buf} = 2 \times 10^{-4}$ mbar.

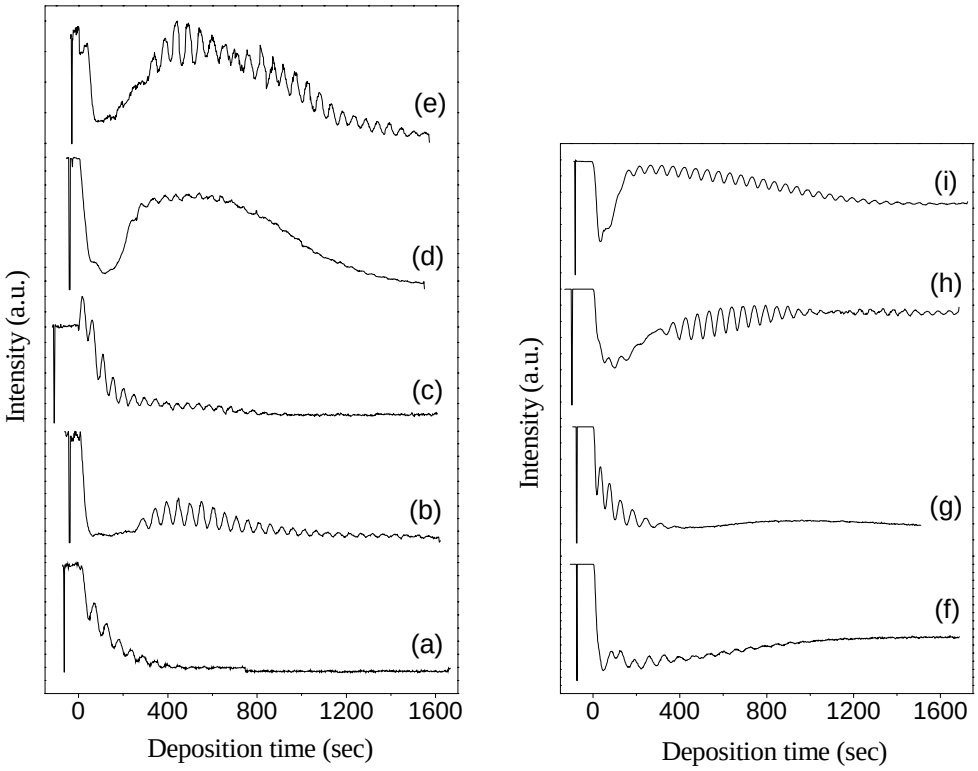

FIGURE 4.11. Oscillations in the intensity of the specularly reflected RHEED beam, as a function of the deposition time of various O_3 assisted samples: (a) grown on MnO substrate at 400°C and $P_{buf} = 1.25 \times 10^{-4}$ mbar, (b) MgO substrate, 400°C and $P_{buf} = 1.5 \times 10^{-4}$ mbar, (c) MnO substrate, 400°C and $P_{buf} = 2 \times 10^{-4}$ mbar, (d) MgO substrate, 400°C and $P_{buf} = 2 \times 10^{-4}$ mbar, (e) MgO substrate, 600°C and $P_{buf} = 2 \times 10^{-4}$ mbar, (f) $SrTiO_3$ substrate, RT and $P_{buf} = 1 \times 10^{-4}$ mbar, (g) $SrTiO_3$ substrate, 400°C and $P_{buf} = 1 \times 10^{-4}$, (h) $SrTiO_3$ substrate, 400°C and $P_{buf} = 1.5 \times 10^{-4}$, (i) $SrTiO_3$ substrate, 400°C and $P_{buf} = 2 \times 10^{-4}$.

The surface becomes rough quite soon for $P_{buf} = 1 \times 10^{-4}$ mbar samples, with polycrystalline features appearing at 400°C, while the sample stays rocksalt at RT. However, the diffraction rods at RT are quite diffuse and the background intensity is relatively high as compared with the NO_2 - assisted samples, indicating probably a not-so-high crystal quality of the sample, or just narrower terraces in this case than

in the NO_2 - assisted samples case. When thicker films are grown at RT with a sample deposition time of $60-90$ minutes (i.e. $\approx 60-90$ ML), then polycrystalline features appear. The samples grown at P_{buf} of 1.5×10^{-4} mbar and 2×10^{-4} mbar are becoming relatively rough in the end of the 30 minutes deposition time.

Figure 4.11 (e) show also the oscillations recorded during the growth of a chromium oxide sample on a $MgO(100)$ substrate, at 600°C, $P_{buf} = 2 \times 10^{-4}$ mbar of O_3 for a deposition time of 30 minutes. The structure of this kind of sample, as determined by RHEED and LEED, will be discussed in the following. We observed that the crystal structure of the sample is changing as a function of the deposition time, in a very similar way as the O_2 - assisted sample grown at 600°C, presented in section 4.2.3 of this chapter. In figure 4.12 the RHEED images are shown of (a) clean MgO substrate, and samples grown in the above conditions, but with different deposition times: (c) 188 seconds (≈ 4 ML) and (e) 30 minutes (≈ 38 ML). The graphs next to the RHEED pictures are plots of the intensity distribution measured along a cross section perpendicular to RHEED streaks in the boxes indicated on each RHEED pattern. The electron beam energy used was 21.2 keV.

After the growth is started, for the first few monolayers, two extra lines are visible in between the rocksalt streaks. They have a weak intensity and are precisely centered in between the rocksalt lines (fig. 4.12 c and d). Later these extra lines disappear, and at around 30 minutes deposition time, the RHEED pattern of the film is similar to the one of the MgO substrate (fig. 4.12 e and f), except that an extra Laue zone below the zeroth order Laue zone is also visible. At this thickness, the film has a relatively flat surface: the RHEED diffraction rods have a streaked character and the RHEED intensity oscillations (see fig. 4.11 e) are still visible. This RHEED pattern remains generally unchanged for deposition times up to 3 hours (i.e. ≈ 240ML), but sometimes when the sample becomes rougher, four extra lines in between the $(\bar{2}, 0)$, (0,0), (2,0) rocksalt lines start to develop. They are placed at exactly one third from the (0,0) - (2,0) lines distance, they remain weak, and have a transmission character, i.e. they look like a bulk signal, just as the ones of the O_2-assisted sample. The extra Laue zone below the zeroth order Laue zone is still visible.

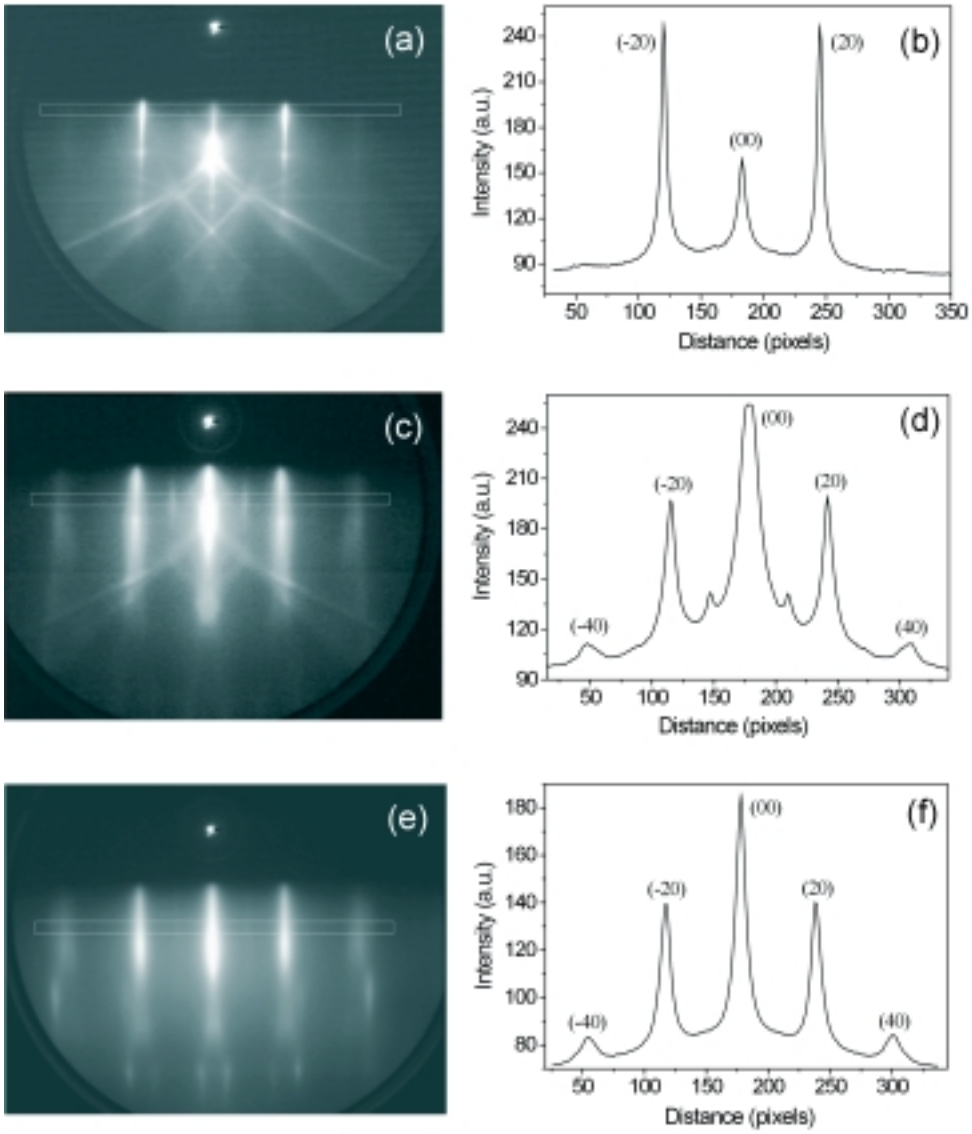

FIGURE 4.12. (a) RHEED pattern of a $MgO(100)$ substrate, (b) horizontal line scan in a box indicated in (a), (c) RHEED pattern of a sample grown on MgO at $600\,^{\circ}$C and $P_{buf} = 2 \times 10^{-4}$ mbar of O_3, after 188 seconds deposition time, (d) horizontal line scan in a box indicated in (c), (e) RHEED pattern after 30 minutes deposition time, (f) horizontal line scan in a box indicated in (e).

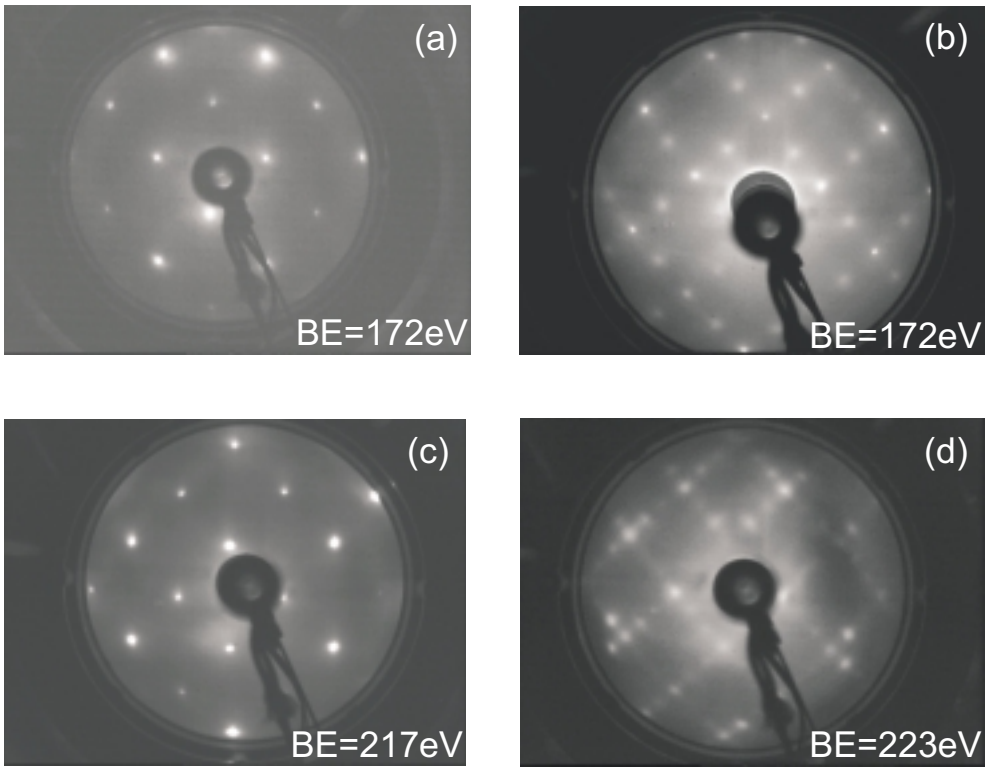

FIGURE 4.13. LEED patterns of (a), (c) $MgO(100)$ substrate, and samples grown on MgO at 600°C, O_3 assisted with $P_{buf} = 2 \times 10^{-4}$ mbar and the deposition times: (b) 188 seconds, (d) 30 minutes. The electron beam energy (BE) is indicated on each figure.

Next, the structure of the samples was checked by LEED and in figure 4.13 the LEED patterns of MgO substrate (a and c) are compared with the patterns of the films at similar electron beam energies (BE) for: (b) 188 seconds deposition time, and (d) 30 minutes deposition time. For the 4 ML sample we noticed a clear (2×1) reconstruction as compared with the MgO pattern, with all the spots having about the same intensity. But for a LEED pattern to be consistent with the RHEED obtained for this sample, it should consist of a (2×2) reconstruction. It is possible that the central spot of the (2×2) in LEED is not visible due to the high background intensity, since it was very weak also in RHEED. The 38 ML sample has a LEED pattern showing two domains of (3×1) and (1×3) reconstructions with respect

to the MgO surface structure. This superstructure is clearly visible, as compared with the O_2 - assisted sample (fig. 4.6 e), and is consistent with RHEED.

Further structural analysis on this kind of sample was done by XRD and RBS measurements and will be presented later in this chapter. It is interesting that this sample deposited at 600°C will keep growing as a single crystal up to 500Å (thicker samples were not tried), while the samples grown at 400°C and $P_{buf} \geq 1.5 \times 10^{-4}$ mbar are developing polycrystalline features starting at $200-250$Å thickness. Probably this is due to the fact that the crystal structure of these samples is a rocksalt defect structure, with ordered chromium vacancies at 600°C (as we discussed for the O_2 - assisted sample), and unordered ones at 400°C, while the oxygen sublattice is in a rocksalt arrangement.

Thick samples can also be grown at 400°C as single-crystals, by growing multilayer samples made up of 5 to 10 units consisting of Cr_xO layers of $\approx 20-30$ ML thickness and MgO spacer layers of 5 ML thickness. RHEED intensity oscillations in the specularly reflected beam for one such multilayer sample are presented in figure 4.14 as a function of deposition time. The sample was deposited in one run, without interruptions in between successive layers, by simultaneously opening and closing the shutters of the Cr and Mg cells, while the O_3 P_{buf} was kept constant, at 2×10^{-4} mbar. During multilayer growth, the RHEED pattern remained rocksalt, with an average intensity decrease during Cr_xO deposition and recovery upon deposition of MgO. The diffraction streaks were slightly more diffuse for the first Cr_xO layer than for the rest of the multilayer sample, probably due to a greater strain of the Cr_xO which is in direct contact with the surface of the substrate. The RHEED intensity oscillations visible up to the fifth Cr_xO layer suggest that the growth mode is layer-by-layer.

If we now look back at all the RHEED intensity oscillations obtained for the O_3 - assisted samples (fig. 4.11), we can try to make a stoichiometry estimation for these samples using the oscillations period. The period for the sample grown on $SrTiO_3$ at RT and $P_{buf} = 1 \times 10^{-4}$ mbar was $62\,\mathrm{sec}/ML$, while for the samples grown at $P_{buf} \geq 1.25 \times 10^{-4}$ mbar the period was in between $51\,\mathrm{sec}/ML$ and $47\,\mathrm{sec}/ML$. If the chemical composition of the film at $P_{buf} = 1 \times 10^{-4}$ mbar is of CrO, then for the rest of the samples it results in a composition in between $Cr_{0.82}O$ and $Cr_{0.76}O$. Further analysis for the samples chemical composition determination was done by XPS measurements and will be presented in the next section.

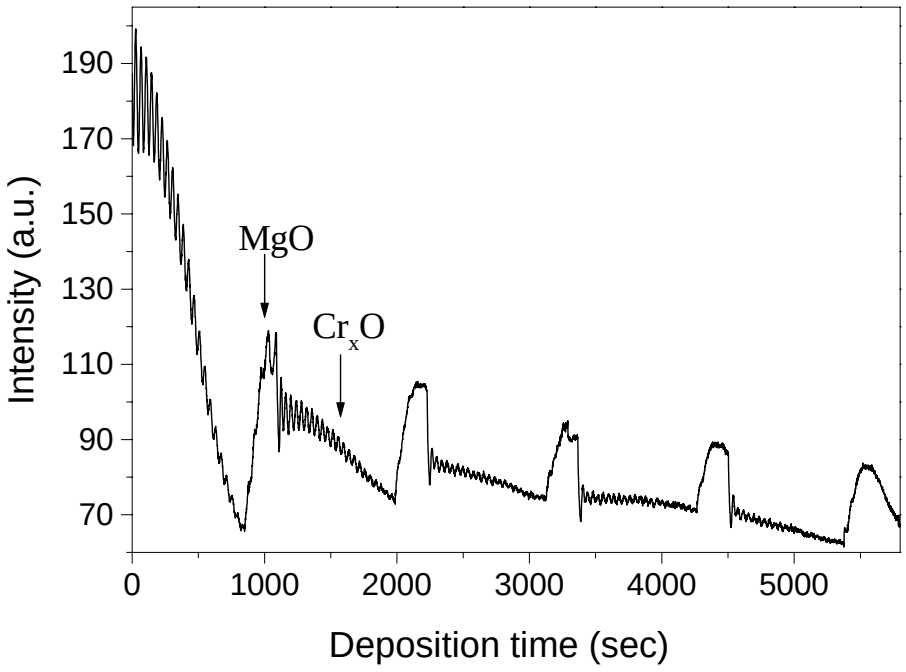

FIGURE 4.14. RHEED intensity oscillations for a Cr_xO/MgO multilayer sample grown on $MgO(100)$ substrate.

4.3.3 XPS results

Chemical composition

The XPS measurements were done in the same way as for the NO_2 - assisted samples. They were started immediately after the growth with a quick broad scan, in which no other peaks except the characteristic chromium and oxygen ones were seen. Then Cr 2p and O 1s core level peaks were measured in the same scan and finally a scan was taken including Cr 3s, Cr 3p, O 2s peaks and the valence band with Cr 3d and O 2p peaks. The chemical composition x of the Cr_xO layers was found from the ratio of Cr 2p and O 1s peak areas, after background subtraction. The reference sample was again the Cr_2O_3 grown on $Al_2O_3(0001)$ presented in section 3.4, with a ratio of Cr 2p vs O 1s of 2.92. The results for the samples

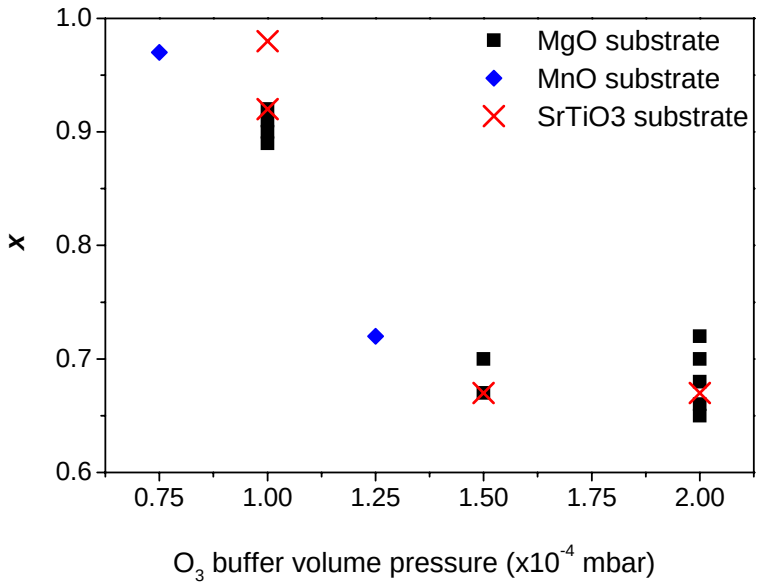

FIGURE 4.15. Chemical composition x of the Cr_xO samples as a function of the O_3 buffer volume pressures as determined from XPS spectra. The reference is Cr_2O_3 grown on $Al_2O_3(0001)$.

previously discussed are presented in figure 4.15 as a function of the O_3 buffer volume pressure.

It can be seen, that x is between 0.67 and 0.72 for $P_{buf} > 1 \times 10^{-4}$ mbar, and that x is close to one for $P_{buf} \approx 1 \times 10^{-4}$ mbar. Recalling the RHEED data results for the sample grown on $SrTiO_3$ at RT and $P_{buf} = 1 \times 10^{-4}$ mbar of O_3, we now seem to have found the correct recipe to make the chromium monoxide: the sample has good crystallinity and a stoichiometry ratio of 1:1 for Cr:O. Further *ex situ* measurements were applied to this type of sample, to complete its characterization.

On the other hand, looking at the Cr 3d vs O 2s ratio for a couple of samples we did not find, for any of the films, the correct value for a 2+ valence of the chromium ion, which should be twice the value for CrO as compared with Cr_2O_3 (see section 3.5.1). Figure 4.16 is a plot of the Cr 3d vs O 2s spectral weights as a function of the O_3 buffer volume pressure used for samples growth.

The Cr 3d peak area was determined by subtracting the O 2p from the total

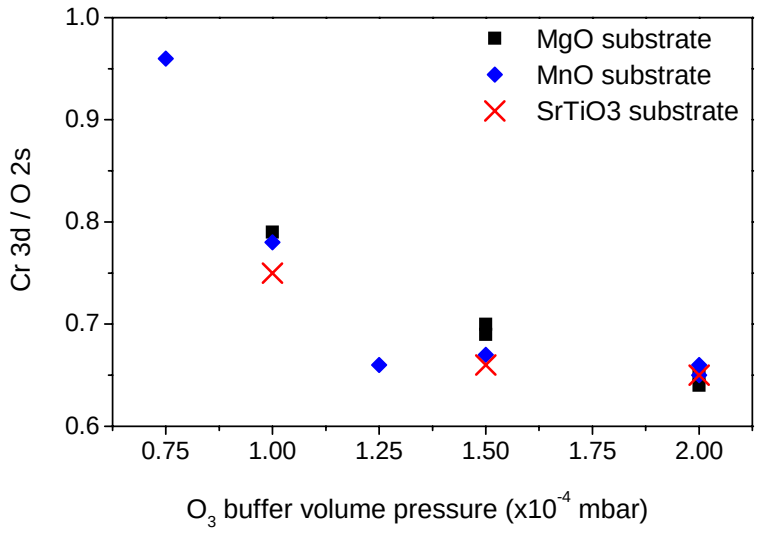

FIGURE 4.16. Cr 3d vs O 2s spectral weights for Cr_xO films as a function of the O_3 buffer volume pressure, as determined from XPS spectra.

(Cr 3d + O 2p) area, where O 2p was found by dividing the O 2s peak area by 2.86, as in the case of the NO_2 assisted samples. The Cr 3d vs O 2s ratio for Cr_2O_3 single crystal is 0.62 and for Cr_2O_3 grown on Al_2O_3 is 0.66. We suspect that for the samples which have a chemical composition close to one Cr to one O this result is not representative due to the post growth oxidation of the films in the XPS chamber, due to the measurement error, and probably due to the different photoionization cross-section per electron for Cr^{3+} and Cr^{2+} ions, as explained in the section 3.5.1.

Electronic structure

Now let us take a brief look at the core level line shapes and chemical shifts of the O_3 assisted samples. Figure 4.17 shows the Cr 2p core level spectra for some of the samples, where the buffer volume pressures used for growing them is indicated on the right side of each line. The reference samples are the Cr_2O_3 single crystal cleaved *in situ* and Cr_2O_3/Al_2O_3 (top), and Cr metal deposited on polycrystalline tantalum (bottom line), as for the NO_2 assisted samples.

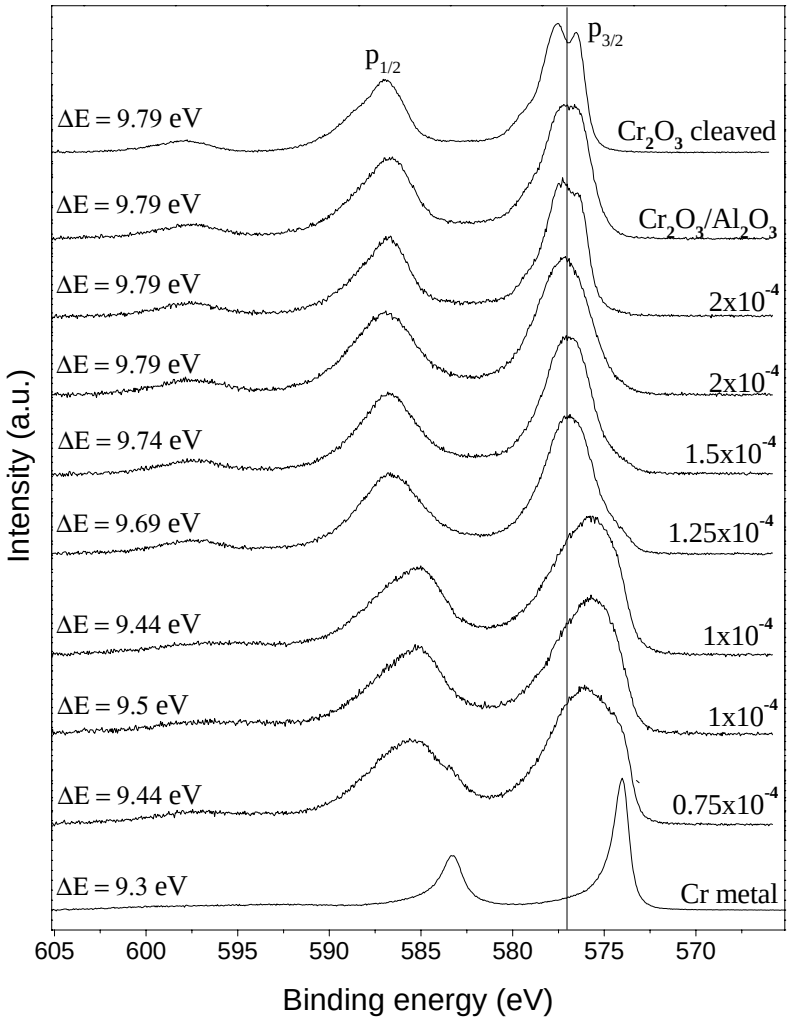

FIGURE 4.17. XPS Al K_α spectra of the $Cr2p$ levels, as a function of the O_3 buffer volume pressures used. P_{buf} (in mbar) is indicated on each spectrum for the grown Cr_xO samples. The lowest spectrum is for the Cr metal deposited on polycrystalline tantalum substrate. The subsequent spectra, from bottom to top, are from samples grown on: MnO(400°C), MgO(400°C), $SrTiO_3$ (RT), MnO(400°C), MgO(400°C), MgO(400°C), MgO(600°C). On the very top there are two spectra for Cr_2O_3: one for a cleaved *in situ* single crystal sample, one for a grown film on $Al_2O_3(0001)$ substrate at $P_{buf} = 12.5 \times 10^{-4}$ mbar of O_2. The spin-orbit energy splitting (ΔE) of the $Cr2p$ is indicated on each spectrum.

The substrates used as we look from the Cr metal to the Cr_2O_3 spectra were: MnO, MgO, $SrTiO_3$ (RT), MnO, MgO, MgO and MgO (600°C). The background was subtracted for each line and the intensities were normalized.

The charge correction was done by using the same method as for the Cr 2p lines of the NO_2 - assisted samples (see section 3.5.2). As a result, the O 1s peak binding energy had the same value for all the chromium oxides, which was: 530.84 eV. Before the correction was done, the O1s BE for the samples grown on MnO and $SrTiO_3$ substrates, for which the use of a flood gun was not needed, was: 530.89 eV for $P_{buf} = 0.75 \times 10^{-4}$ mbar sample, 531.04 eV for $P_{buf} = 1 \times 10^{-4}$ mbar sample, and 530.49 eV for $P_{buf} = 1.25 \times 10^{-4}$ mbar sample, values which are all very close to 530.84 eV, the after charge correction BE value.

The sample grown at $P_{buf} = 0.75 \times 10^{-4}$ mbar has a very broad and asymmetric Cr $2p_{3/2}$ line which is probably due to a mixture of Cr metal and some oxide of chromium. For the samples grown at $P_{buf} = 1 \times 10^{-4}$ mbar the $2p_{3/2}$ lines are also broad, but they have a relatively symmetric shape. The samples grown at $P_{buf} \geq 1.25 \times 10^{-4}$ mbar have Cr 2p line shapes very similar to the ones of Cr_2O_3 samples, and moreover, the peaks positions seem to coincide with the ones of Cr_2O_3 samples. In the following table the Cr $2p_{3/2}$ binding energies are given for the spectra from fig. 4.17, together with the shifts in BE relative to the Cr $2p_{3/2}$ peak position of Cr metal, 574.02 eV, obtained after the charge correction for all the samples. For comparison some values taken from reference [2], [3], [4] and [5] are included.

Looking at the BE shifts it seems that for the samples grown at $P_{buf} = 1 \times 10^{-4}$ mbar chromium ion has a 2+ valence state, while for the samples grown at $P_{buf} \geq 1.25 \times 10^{-4}$ mbar the valency of the chromium seems to be 3+. The sample grown at $P_{buf} = 0.75 \times 10^{-4}$ mbar is not listed in this table, since the Cr $2p_{3/2}$ peak is strongly asymmetric.

Figure 4.17 also indicates the spin-orbit splitting energy ΔE, on the left side of each spectrum. The ΔE values obtained for the samples grown at $P_{buf} = 1 \times 10^{-4}$ mbar, together with the BE shifts, suggest that chromium has a 2+ valence state in these samples [6].

Figure 4.18 shows the Cr 3p and 3s spectral lines for the same samples used in figure 4.17. The background was subtracted for each graph, the intensities were normalized, and the spectra were charge corrected using the same method as for the Cr 2p lines. The correspondent buffer volume pressure is indicated on each graph for the grown samples.

P_{buf} (mbar)	Cr $2p_{3/2}$ BE (eV)	BE shifts as compared with Cr metal
1×10^{-4}	575.81	1.79
1×10^{-4}	575.87	1.85
1.25×10^{-4}	577.02	3
1.5×10^{-4}	577.01	2.99
2×10^{-4}	577.27	3.25
2×10^{-4}	576.96	2.94
Cr_2O_3/Al_2O_3	577.02	3
Cr_2O_3 single crystal	576.96	2.94
ref. [3] Cr^{3+}	577.2	3.2
ref. [2], [4], [5] Cr^{3+}	577	2.8
ref. [2], [4], [5] Cr^{2+}	576	1.8

The Cr 3p lines of the samples grown at $P_{buf} \leq 1 \times 10^{-4}$ mbar have a double peak structure with a feature to low BE which seems to have the same position as the Cr 3p peak of metal, and a feature at higher BE having about the same position as the Cr 3p peak of Cr_2O_3. For the films which did not grow as single - crystals, this fact could be an indication of a phase mixture of Cr metal and the stable Cr_2O_3 phase. On the other hand, looking at the spectra of the sample grown epitaxial on $SrTiO_3$ at RT, it could be that this is the characteristic shape of the Cr 3p line for chromium monoxide, in which non-local screening effects may play an important role due to the very much increased intersite hopping either via direct Cr-Cr or via 180° Cr-O bond. The sample grown at $P_{buf} = 1.25 \times 10^{-4}$ mbar has a Cr 3p line with a low intensity shoulder at smaller BE, while the Cr 3p line shapes of the samples grown at $P_{buf} \geq 1.5 \times 10^{-4}$ mbar look very similar to Cr_2O_3 ones and have about the same peak position.

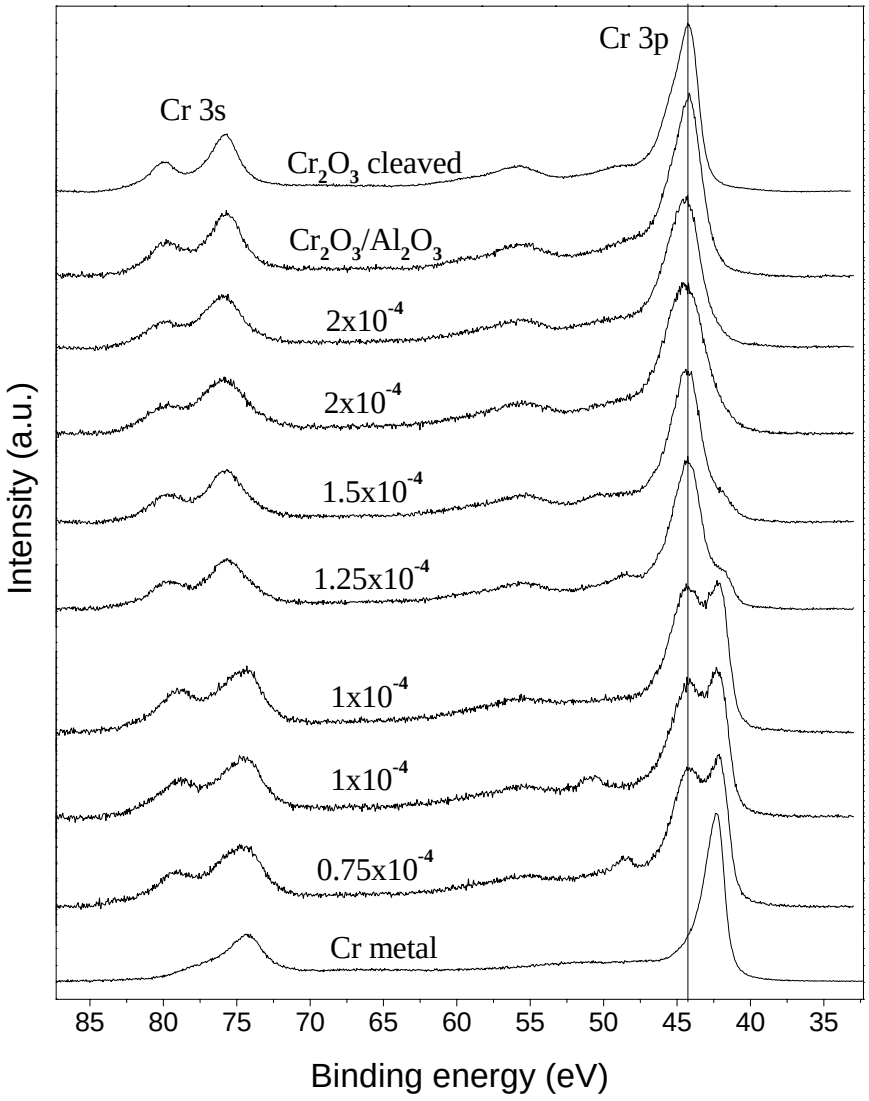

FIGURE 4.18. XPS Al K_α of the $Cr3p$ and $Cr3s$ levels, as a function of the O_3 buffer volume pressures used. P_{buf} (in mbar) is indicated on each spectrum for the grown Cr_xO samples. The lowest spectrum is for the Cr metal deposited on tantalum substrate. The subsequent spectra, from bottom to top, are from samples grown on: MnO, MgO, $SrTiO_3$ (RT), MnO, MgO, MgO, MgO (600°C). On the very top there are two spectra for Cr_2O_3: one for a cleaved *in situ* single crystal sample, and the other one for a grown film on $Al_2O_3(0001)$ substrate at $P_{buf} = 12.5 \times 10^{-4}$ mbar of O_2.

We made also an attempt to determine for these O_3 assisted samples the Cr 3s exchange splitting energy and the spectral weights ratio of the two peaks by fitting the Cr 3s lines, and the results are presented in the next table. However, as in the NO_2 - assisted sample case, the reliability of the fitting may not be very good, since the Cr 3s peaks are broad.

P_{buf} (mbar)	Exchange splitting energy (eV)	Cr 3s weights ratio
0.75×10^{-4}	4.46	1.55
1×10^{-4}	4.43	1.25
1×10^{-4}	4.28	1.33
1.25×10^{-4}	4.08	2.35
1.5×10^{-4}	4.14	2.43
2×10^{-4}	4.24	2.73
2×10^{-4}	4.1	2.3
Cr_2O_3/Al_2O_3	4.1	2.01
Cr_2O_3 single crystal	4.1	2.18

The exchange splitting energy expected for Cr^{3+} ion is ≈ 4.2 eV [7], [8] and ≈ 5 eV for Cr^{2+} ion [9], [10].

Next, figure 4.19 shows the VB together with the O 2s spectra, for the same samples used in figures 4.17 and 4.18, as well as the spectrum for a $MgO(100)$ annealed substrate for comparison. The background was subtracted for each spectrum, all the intensities were normalized and they were charge corrected using the same method as for the Cr 2p lines.

We will end this section with a last remark on a check which was done for the samples grown at 600°C on MgO. We studied whether or not Mg from the substrate is intermixing with Cr_xO at this high temperature, resulting perhaps in a Cr_2MgO_4 spinel - like compound. We have measured the Mg 2s peak on chromium oxide samples of different thickness: 4 ML, 9 ML and 38 ML. Its signal was found to decrease exponentially with the thickness of the film. This means that there is indeed no Mg intermixing and that Cr_xO is indeed growing in a layer by layer mode.

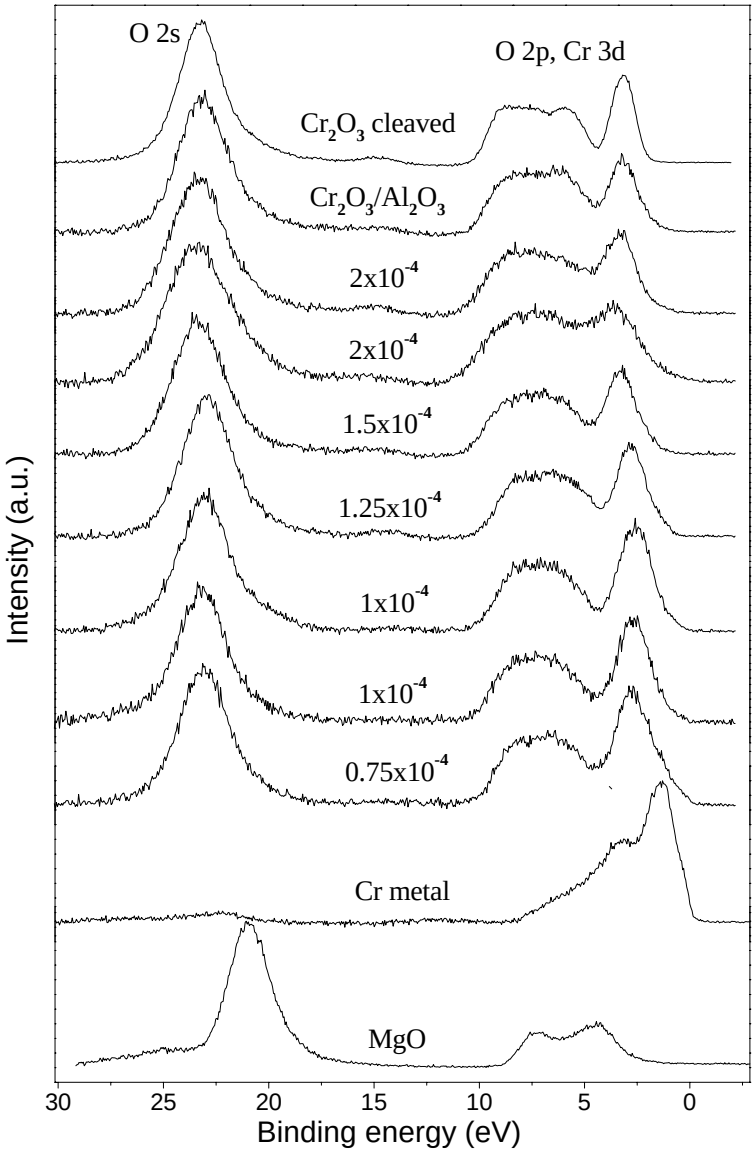

FIGURE 4.19. XPS Al K_α of the VB and $O2s$ levels, as a function of the O_3 buffer volume pressure used. P_{buf} (in mbar) is indicated on each spectrum for the grown Cr_xO samples. The lowest spectrum is for the MgO annealed substrate, then the Cr metal deposited on tantalum substrate spectrum and subsequently the samples grown on: MnO, MgO, $SrTiO_3$ (RT), MnO, MgO, MgO, MgO (600°C). On the top there are two spectra for Cr_2O_3: one for a cleaved *in situ* single crystal sample, and the other one for a grown film on $Al_2O_3(0001)$ substrate at $P_{buf} = 12.5 \times 10^{-4}$ mbar of O_2.

4.3.4 *Ex situ* structural analysis

For the *ex situ* measurements we have used the two most interesting samples from the O_3 - assisted ones: a sample grown on MgO at 600°C and 2×10^{-4} mbar of O_3, and a sample grown on $SrTiO_3$ at RT and 1×10^{-4} mbar O_3. The first type of sample seemed to have an ordered defect structure with a two domain reconstruction (3×1) and (1×3) with respect to the MgO substrate structure, and a chemical composition of approximatively $Cr_{0.7}O$. Relatively good single crystals could be grown in these conditions with thickness varying between 75 and 500Å. The second type of sample showed a rocksalt structure in RHEED for a maximum thickness of 130-190Å, and has a chemical composition of CrO, being the only sample found with this desired chemical composition and having a relatively good crystal structure.

RBS

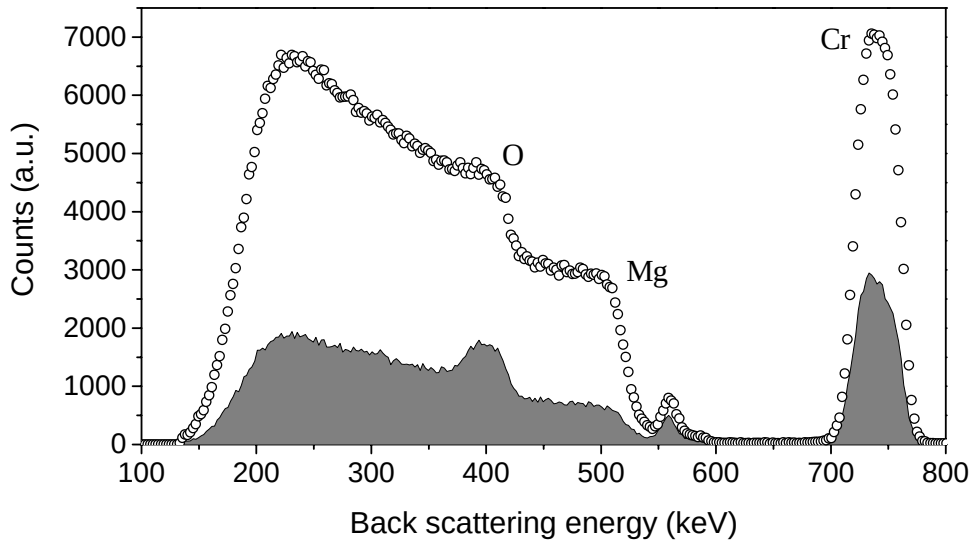

FIGURE 4.20. RBS spectra for random direction (circles) and [001] aligned orientation (filled area) for the sample. The minimum yield is 41%.

Two RBS spectra[1] are shown in figure 4.20, measured on a $Cr_{0.7}O$ sample grown on MgO substrate, with a thickness of $\approx$ 330Å. The filled area represents the spectrum taken with the ion beam incident along the [001] crystal axis of MgO substrate, and the circles represent the spectrum measured for a random direction of the beam. The chromium, magnesium and oxygen edges are indicated on the random spectrum. The minimum yield in the channelled direction is about 41%, revealing that the vacancies in the bulk are not so ordered. The magnesium intensity peak in the channelling direction spectrum originates from the surface of the MgO cap layer. Due to this cap layer, no reliable stoichiometry determinations could be done with RBS.

Even more surprising is the result of the same measurement done on CrO films grown on $SrTiO_3$. In this case RBS showed no channelling for CrO along the [001] or [011] crystal axis, the intensity of the chromium peak was found to be the same for the random spectrum as for the channelling direction. The result is the same for two samples with different thicknesses: one of 64Åand the other one of 160Å. This indicates that a considerable amount of disorder is present in these samples.

XRD

XRD was used to check the structure of the two types of samples[2]. Figure 4.21 is an areal XRD picture of the $Cr_{0.7}O$ sample grown on MgO substrate, and it confirms the RHEED data results, that the superstructure of the film is in fact not a surface structure, but a bulk structure. This k-space picture is based on a series of $\theta - 2\theta$ scans for different tilt angles of the sample with respect to the reflection plane (a series of $\omega - 2\theta$ scans in a range of ψ values). The intensity scan is logarithmic and the axes (in-plane $k_{||}$ and out-of-plane $k_{\perp}$ reciprocal wave vectors) are in the units of $2\pi/\lambda$ with $\lambda = 0.15418$ nm. The vertical axis is perpendicular to the surface and the horizontal axis is in the [110] direction.

The intense (indexed) spots originate from the substrate and the weak superstructure spots from the $Cr_{0.7}O$ film. Figure 4.22 is a schematic drawing of the reconstructed XRD picture where the black filled circles correspond to the initial rocksalt diffraction spots of the MgO substrate, and the grey filled circles and the open circles are the superstructure spots.

[1] These RBS measurements have been performed by S. Grachev.
[2] These XRD measurements have been performed in the group of T. Hibma.

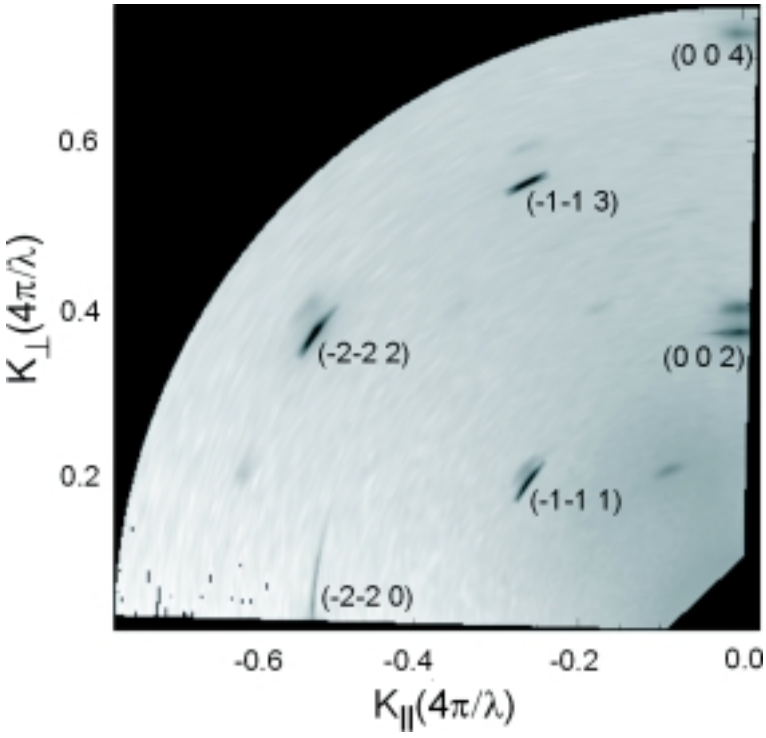

FIGURE 4.21. Areal XRD picture of a 330Å thick $Cr_{0.7}O$ sample grown $MgO(100)$ film, capped with 40Å of MgO. The horizontal axis is the in-plane [110] direction. The reciprocal wave vectors $k_{\|}$ and $k_{\perp}$ axis are in the units of $2\pi/\lambda$ with $\lambda = 0.15418$ nm.

The unit cell of the film structure is a body centered orthorhombic unit cell with lattice parameters $a = a_{MgO}/\sqrt{2}$, $b = 3a_{MgO}/\sqrt{2}$ and c somewhat smaller than a_{MgO}. The cell size therefore is about 1.5 times as large as a MgO unit cell. A structure consistent with this unit cell is one in which the ions occupy similar sites as in the rocksalt structure, with one out of each three chromium sites being vacant in an ordered way.

For the CrO film grown on $SrTiO_3$ we found just (00l) sharp strong peaks, indicating that there is order in the c direction of the CrO crystal, but there is very little order in the (ab) plane. This confirms the RBS result, but it is also a serious problem since from the RHEED and XPS data point of view these were the best

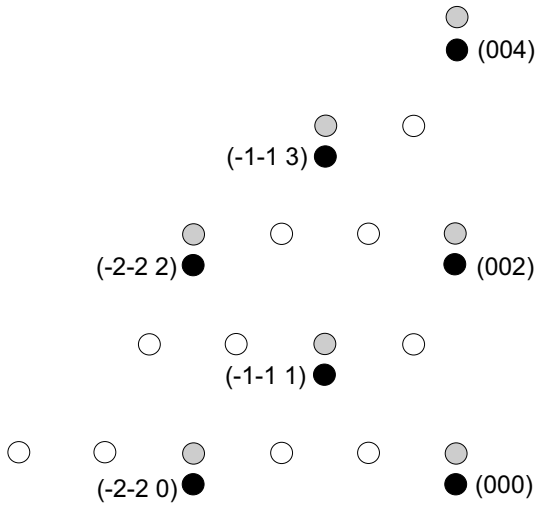

FIGURE 4.22. Schematic drawing of the reconstructed XRD picture.

conditions found for growing crystalline samples with the chemical composition of chromium monoxide. Nevertheless, we will give here the found lattice constants in plane: $a = b \approx 4.16$Å, as determined from the RHEED lines separation of CrO compared with the ones of $SrTiO_3$ substrate, and out of plane: $c \approx 4.26$Å, as determined from the XRD, where $c = \frac{\lambda}{\sin\theta}$, with λ is the wavelength of the radiation and θ is the diffraction angle. So, the "ordered" part of the CrO crystal seems to have a rocksalt tetragonally distorted structure.

In principle, one can determine the stoichiometry of the grown samples from fits of the reflectivity scans in XRD. One of the parameters needed for fitting these spectra is the electronic density of the samples, which varies for the different chromium oxides. The values found for x are consistent with those found by XPS, but they were less accurate, so we stay with the stoichiometry determination by XPS as our method of choice.

4.3.5 XAS results

Finally, the two types of sample O_3 - assisted mentioned above were measured by XAS in order to find out what the valency is of the chromium ion.

Figure 4.23 shows the Cr L_{23} TEY X-ray absorption spectra of: a CrO sample $\approx$ 64Å thick, grown on the $SrTiO_3$ at RT and $P_{buf} = 1 \times 10^{-4}$ mbar of O_3 (bottom line), and a $Cr_{0.7}O$ sample $\approx$ 70Å thick grown on MgO at 600°C and $P_{buf} = 2 \times 10^{-4}$ mbar of O_3 (middle line). The spectrum of a Cr_2O_3 single crystal sample cleaved *in situ* (top line) is included for comparison. The spectra of the films are taken both at normal incidence (continuous lines) and grazing incidence (dotted

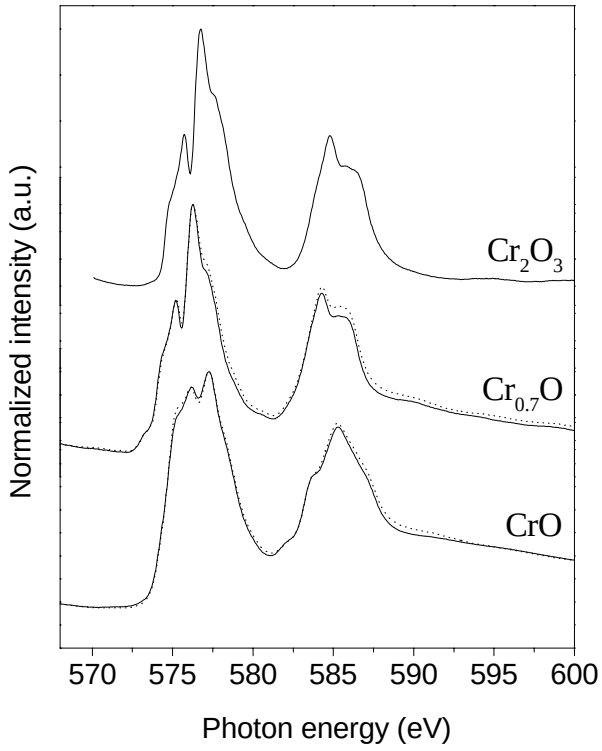

FIGURE 4.23. CrL_{23} TEY X-ray absorbtion spectra of: Cr_2O_3 cleaved sample (top) and two grown chromium oxides samples: $SrTiO_3(100)$ substrate, RT, 1×10^{-4} mbar of O_3 (bottom) and $MgO(100)$ substrate, 600°C, 2×10^{-4} mbar of O_3 (middle).

lines). The intensities were normalized for each spectrum, to the peak maximum.

It can be seen that the spectrum of the $Cr_{0.7}O$ sample looks very similar to the one of the Cr_2O_3 reference, which indicates that all the chromium ions are in a 3+ valence state. On the other hand, the CrO sample has a spectral line shape which differs from the one of Cr_2O_3, and fitting of this spectrum indicated that most of the chromium ions are in a 2+ valence state. But there is basically no difference between the normal incidence spectrum and the grazing incidence one, as it should be in the case of a d^4 ordered Jahn-Teller system. This is not surprising in view of the fact that a substantial amount of disorder was found in the crystal structure of this type of sample.

4.4 Conclusions

In conclusion we can grow chromium oxide films Cr_xO on various substrates (MgO, MnO, and $SrTiO_3$), with chemical composition x ranging from 1 to 0.67.

For low O_3 pressure, the chromium oxide sample grown on $SrTiO_3$ at RT has a chromium to oxygen ratio which is close to one. XAS reveals that the Cr valence is close to 2+ in this case. The crystal structure is rocksalt fcc, as seen by RHEED, but there is a substantial amount of disorder: with XRD measurements we found no crystalline order in the (ab) plane of the CrO crystal, and RBS measurements showed no channelling of the ion beam for the film. We suspect that this is closely related to the Jahn-Teller distortion that should occur for a system that contains Cr^{2+} $3d^4$ ions, distortions which are not ordered. This conclusions is supported also by XAS measurements where we found no dichroism, as one would expect for an ordered type of Jahn-Teller system.

For high gas (O_2 or O_3) pressures the chromium oxide has a composition approximately of $Cr_{0.7}O$ and a rocksalt crystal structure seen by RHEED, if the samples were grown at 400°C. We believe that in fact just the oxygen sublattice has a rocksalt - like arrangement, while in the chromium sublattice vacancies are present in an unordered way, which in RHEED appears as an increased background intensity. Nevertheless, the defects in the chromium sublattice seem to become ordered when the substrate temperature is increased above 600°C, and the defect rocksalt fcc structure shows a (3×1) superstructure with respect to the $MgO(100)$ surface in RHEED, LEED and XRD.

The crystal quality of the samples grown with NO_2 is better than of the samples grown with O_2 or O_3, as seen by RHEED, XRD and RBS. Also the films seem to have an increased surface roughness if they are O_2 - assisted, as compared with the O_3 - assisted ones.

Chromium oxide samples with similar chemical compositions are grown for equal flux of any of the three oxidizing agents used, so we can conclude that in our system NO_2, O_2 and O_3 have about the same oxidizing power (efficiency) for chromium oxide growth.

References

[1] F.C.Voogt, PhD thesis, University of Groningen, The Netherlands (1998).
[2] C. Xu, M. Hassel, H. Kuhlenbeck, H.J. Freund, Surf. Sci. **258**, 23 (1991).
[3] A.M. Venezia, C.M. Loxton and J.A. Horton, Surf. Sci. **225**, 195 (1990).
[4] A. Maetaki, M. Yamamoto, H. Matsumoto and K. Kishi, Surf. Sci. **445**, 80-88 (2000).
[5] A. Maetaki and K. Kishi, Surf. Sci. **411**, 35-45 (1998).
[6] R. Marryfield, M. McDaniel and G. Parks, J. Catal. **77**, 348 (1982).
[7] T.A. Carlson, J.C. Carver, L.J. Saethre, F.G. Santibanez and G.A. Vernon, J. El. Spectr. Rel. Phenomena **5**, 247 (1974).
[8] S. Altieri, PhD thesis, University of Groningen, The Netherlands (1999).
[9] C.S. Fadley, Electron Spectroscopy, ed. D.A. Shirley (North-Holland, Amsterdam), 781 (1972).
[10] D.A. Shirley, Topics in Applied Physics, Photoemission in Solids I, ed. M. Cordona and L. Ley (Springer-Verlag, Berlin), 165 (1978).